INFRARED METHODS FOR DAYLIGHT ACQUISITION OF LEO SATELLITES

THESIS

Joel E. Nelson, Captain, USAF

AFIT/GSS/ENG/04-02

DEPARTMENT OF THE AIR FORCE
AIR UNIVERSITY

AIR FORCE INSTITUTE OF TECHNOLOGY

Wright-Patterson Air Force Base, Ohio

The views expressed in this thesis are those of the author and do not reflect the official policy or position of the United States Air Force, Department of Defense, or the United States Government.

AFIT/GSS/ENG/04-02

INFRARED METHODS FOR DAYLIGHT ACQUISITION OF LEO SATELLITES

THESIS

Presented to the Faculty

Department of Electrical and Computer Engineering

Department of Aeronautics and Astronautics

Graduate School of Engineering and Management

Air Force Institute of Technology

Air University

Air Education and Training Command

In Partial Fulfillment of the Requirements for the

Degree of Master of Science in Aerospace and Information Operations

Joel E. Nelson, BS

Captain, USAF

March 2004

AFIT/GSS/ENG/04-02

INFRARED METHODS FOR DAYLIGHT ACQUISITION OF LEO SATELLITES

Joel E. Nelson, BS
Captain, USAF

Approved:

/signed/

Matthew E. Goda (Chairman) date

/signed/

Ronald F. Tuttle (Member) date

/signed/

Richard G. Cobb (Member) date

Acknowledgments

Wow, what a great opportunity to explore different aspects of God's creation. Essentially this work focuses on the study of the "light" He created, and no better place existed to conduct the work than the Maui Space Surveillance Site. I would like to thank my wife for all her support and encouragement. This has been an exciting adventure to share with you! Without the efforts of Lt Col Brent Richert, Maj Dave Lee, Dr. Chris Sabol, and Maj Matt Goda, none of this research would have occurred. Thanks to each of you. In addition, Paul Sydney, Dan O'Connell, and Mike Murai proved to be great teachers and partners in this developmental research. Good luck, guys, with the LEO Raven prototype. I hope you enjoy reading this exploration of "light" and how to better use it for National Security.

Joel E. Nelson

Table of Contents

List of Figures

Page

List of Tables

Page

Abstract

Raven is an award-winning optical system design paradigm that couples commercially available hardware and software along with custom data analysis and control software to produce low-cost, autonomous, and very capable space surveillance systems. The first product of the Raven program was a family of telescopes capable of generating world-class optical observation data of deep-space satellites. The key to this system was the use of astrometric techniques for position and brightness data. Astrometry compares a satellite to the star background within the sensor field of view; since the position and brightness of the star-field is well known in star catalogs, accurate knowledge of the satellite position and brightness can be deduced from this comparison. Efforts are now underway to produce a similar system capable of tracking low Earth orbiting (LEO) satellites: the LEO Raven. Tracking LEO objects presents several new challenges, most notably the speed of the satellite relative to the star-field and the lighting conditions. The current system works in the visible light band that requires terminator tracking conditions where the ground station is in the dark and the satellite is solar illuminated. Since this is not typically the case for LEO satellites, the first LEO Raven is being designed to use infrared light bands for daylight tracking. This thesis presents the results of risk-reduction daylight astrometry experiments using the Maui Space Surveillance Site's Daylight Acquisition Sensor.

INFRARED METHODS FOR DAYLIGHT ACQUISITION OF LEO SATELLITES

I. Introduction

1.1 Background

Since the Maui Space Surveillance Site (MSSS) was turned over to the Air Force Research Laboratory (AFRL) from Air Force Space Command (AFSPC) in 2000, the focus shifted to research and development. To uphold Department of Defense research and operational goals, MSSS develops potential force enhancing systems relating to the space surveillance mission area, which include the Raven-class telescopes. Plans for a High Accuracy Network Determination System (HANDS) utilizing the Raven-class telescope exist to further solidify MSSS's contributions to the intelligence and space community. A piece of this program is to provide accurate orbit determination.[1]

Raven is an award-winning optical system design paradigm that couples commercially available hardware and software along with custom data analysis and control software to produce low-cost, autonomous, and very capable space surveillance systems.[2] The first product of the Raven program was a family of telescopes capable of generating world-class optical observation data of deep-space satellites, but now efforts are underway to produce a similar system capable of tracking low Earth orbiting (LEO) satellites: the LEO Raven. Tracking LEO objects presents several new challenges, most notably the speed of the satellite

relative to the star-field and the lighting conditions. The current system works in the visible light band that requires terminator tracking conditions where the ground station is in the dark and the satellite is solar illuminated. Since LEO satellites rarely over-fly with terminator conditions, LEO Raven may be required to use infrared light bands for daylight tracking.

Previous work has shown that high accuracy angles data can have a significant impact on low earth orbit determination and prediction accuracy.[3,4] These works have relied on large and expensive telescope systems to provide angular observation data. Raven class telescopes have shown the ability to capture arcsecond level angular observations of geosynchronous satellites and analysis has shown that observations of this quality are extremely valuable in the orbit determination process.[5,6] As impressive as the original Raven telescopes and their uses for deep space satellite surveillance are, a LEO Raven could have a much larger impact. The LEO Raven concept provides a potentially inexpensive yet effective method to generate high accuracy track metrics and photometry for LEO satellites outside of terminator.

1.2 Problem Statement

Space surveillance products from Air Force Space Command (AFPSC) have not been accurate enough for certain applications, specifically acquisition and/or illumination of dark satellite passes. In addition, current Ground-Based Electro-Optical Deep Space Surveillance (GEODSS) operate only at night which severely limits 24 hour coverage in the event of a daytime space launch, daytime maneuver, or spacecraft related problem. While orbit determination methods have been refined for geosynchronous (GEO) satellites, a system must

be developed to monitor LEO satellites. A solution for this problem is using high accuracy orbit updates from a Raven-type system. These orbit updates require filter techniques to update orbital elements using a single pass of metric data and catalog maintenance which focuses on achieving required accuracy for all satellites. Customers for this type of AFSPC capability include the Air Force Research Laboratory (AFRL) Active Track program, AMOS LWIR Imager, and Missile Defense Agency (MDA) to name a few.[1] This method would also prove to be a low cost but highly accurate method of orbit determination to support Space Object Identification (SOI) and other missions.

1.3 Research Objectives

The Raven design paradigm does not start with rigid performance specifications; rather the challenge is to determine what can be accomplished with commercially available components. For LEO Raven, this manifests itself in the following way: given today's commercially available CCD cameras (IR and visible) and a 0.5m telescope, can we do daylight astrometry for low-Earth orbiting satellites? If so, what can we see?

The trade space for the design study includes available camera specifications and telescope field of view (FOV). A large FOV makes more stars available for the astrometric processing; however, this increases the requirement on the CCD camera to provide enough sensitivity to detect objects above the sky background. Perhaps a 1m class telescope is required to support the concept? This thesis presents the results of risk-reduction experiments and engineering studies that will assist in the design and capability projection of the LEO Raven.

Particular issues addressed are summarized in Table 1.

Table 1. Research Questions

1	Objects move much faster in LEO which presents field-of-view and imaging duration challenges. Question: Can the system track fast enough for LEO objects?
2	Observations will need to occur in the 1-1.5 micron range (near-infrared or NIR), effectively "filtering" out the blue sky. Question: Can an adequate number of stars be seen, above the sky background, in a single field-of-view in order to accomplish the astrometry?
3	What characteristics will be essential in a NIR camera and telescope system to be used for daylight observations? Is the current Merlin camera and Raven telescope configuration adequate? What improvements are possible with a different detector?
4	Finally, given the answers to these questions, can an accurate system model be created in order to scale the results to the parameters of a future deployable LEO Raven?

These questions will be explored and answered in Chapter 5.

Radiometric models along with an understanding of astrometric requirements are needed to explore this trade space. These models can be developed using various levels of detail. A key to determining the utility of these models is to anchor them using results from real data collections. Once a model is validated, it can be applied to potential LEO Raven system configurations to project capabilities and determine which, if any, of the designs are worth fielding. Figure 1 illustrates this process; the thesis focus areas are shaded in gray.

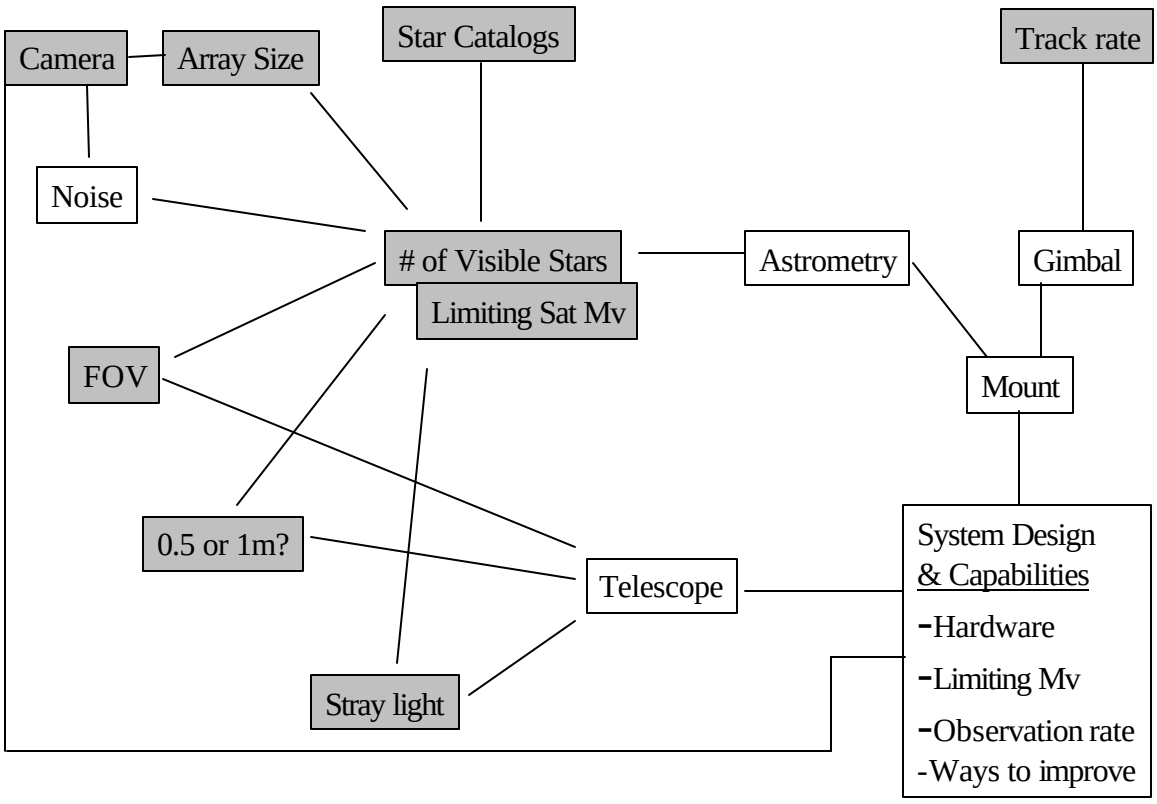

Figure 1. LEO Raven Design Description

The forthcoming analysis and recommendations will serve as risk reduction for the final design of the deployable LEO Raven system.

1.4 Research Approach

Building on deep space astronomy observation techniques, this application will champion astrometric techniques for LEO space object identification and explore the appropriate telescope set up and infrared sensor requirements. Preliminary experiments utilize the 0.42m HANDS Raven telescope for exploration of the telescope tracking capabilities.

Next, data will be collected with the Maui Space Surveillance Site's Daylight Acquisition System (DAS) on the 1.6m GEMINI telescope. This collection will hopefully provide enough star/satellite data to perform astrometry. In addition, experiments will be conducted on the 0.36m Remote Maui Experiment (RME) Raven configured with the DAS or Merlin camera. This data will help explain the capabilities and limitations of the current Raven/IR camera combination. Aspects of this research include finding satellite targets of interest, choosing the appropriate NIR sensor for use during daylight, evaluating source star densities in the NIR, and exploring the LEO Raven design trade space. With sufficient risk reduction data from the DAS experiments, a final recommendation will be made on parameters for a prototype LEO Raven system.

This research faces several challenges at the outset. These limitations are summarized in the Table 2.

Table 2. Limitations

Weather constraints on observations (to include clouds, wind, and humidity)
Software challenges with camera and telescope operation
Mount time on the various telescopes due to competing priorities with AFSPC, AFRL, and MDA
Sky background brightness during the daylight
Time constraints for experimentation due to AFIT requirements
Current field-of-views of the various telescopes (Will enough stars be seen for the astrometry?)
Speed of LEO satellites and the capability of the mount tracking
Time tagging of the data in order to get accurate position data
Sensitivity of the current Indigo Merlin (DAS) infrared detector

Despite these limitations, the research at the Maui Space Surveillance Site provided adequate data to guide the final recommendations for the LEO Raven prototype. Once this deployable LEO Raven enters operation, several beneficial implications exist for AFRL and AFSPC. Section 1.5 outlines these research implications.

1.5 Research Implications

This thesis research supports Air Force Research Laboratory efforts and Space Command operational space surveillance missions. A LEO Raven system will provide high accuracy metrics and photometry for LEO satellites outside of terminator. This supports space object identification, threat assessment, and anomaly resolution. In addition, this system would increase size of neighborhood watch for space system protection and add capabilities to search for new, lost, or maneuvering objects. [7]

1.6 Preview

The following methodology, research, and analysis will explain what was accomplished through the three-pronged approach to designing a deployable, daylight LEO Raven system. The systems—the 0.42m HANDS, 1.60m GEMINI, and 0.36m RME Raven—and the software tools will lay the ground work for the LEO Raven design. Chapter 2 discusses background knowledge and reviews topics germane to understanding the end-to-end analysis approach—following photons from the star or satellite, through the atmosphere, optical system,

detector, and finally to the detector output signal. Chapter 3 explores the experimentation methodology, expounding on the end-to-end photon study. Chapter 4 discusses the experiments conducted, challenges encountered, and atmospheric, radiometric, and astrometric analyses accomplished. Finally, chapter 5 addresses the answers to questions posed in section 1.3, and presents concluding thoughts, and recommendations for future LEO Raven experiments.

II. Background Theory

The following material consists of the literature reviewed for an understanding of the end-to-end process following photons leaving a source (the sun or stars) to their arrival at the detector. Each step will be described in greater detail in the following sections. The process starts with observed electromagnetic radiation from stars. For the cases presented in this thesis, stars are either directly observed or seen via reflections off a satellite or the atmosphere. In the case of targeted satellites, discussions of reflection aid in understanding the radiation coming from a satellite which is characteristic of sunlight. Next, different star properties will be discussed to include brightness scales and spectral class. Since stars emit radiation at different temperatures, their observed radiation will differ from star to star. This must be understood in order to better conduct and explain this research. Once radiation from either a star or reflected from a satellite reaches the top of the Earth's atmosphere, not all of it will pass through to the surface. To fill in this part of the end-to-end process, background information in atmospheric transmission is presented. Once the incident radiation reaches the telescope still more losses are introduced due to the reflective and refractive optics. Finally, the photons reach the detector and are converted to digital counts which are displayed in the software. Each of the steps in this end-to-end process must be understood in order to build an effective LEO Raven system.

2.1 Electromagnetic Radiation

No discussion of infrared technologies would be complete without a discussion of electromagnetic radiation in general. Electromagnetic theory lays the foundation for IR technologies and the resulting detectors. Radiation can be categorized by its wavelength or frequency and includes radio waves, ultraviolet rays, X-rays, visible light, and infrared radiation. The Figure 2 relates different radiation types to the corresponding frequency and wavelength.

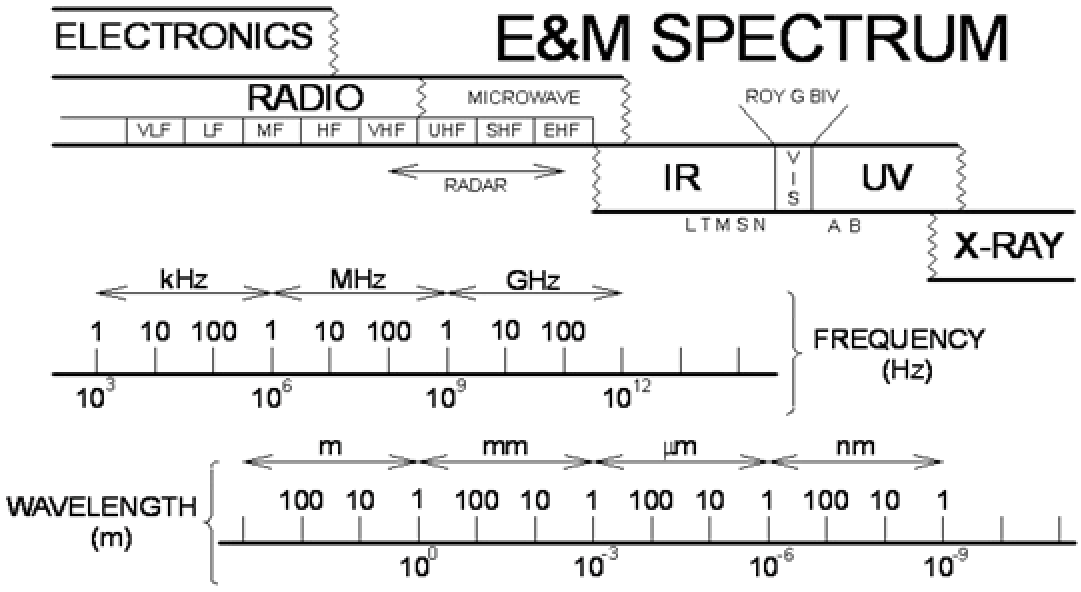

Figure 2. Electromagnetic Spectrum[8]

Visible light ranges from the violet at 0.4 micrometers to 0.7 micrometers in the red. The infrared radiation bands extend within the electromagnetic spectrum between 0.7 micrometers and 350 micrometers. Although many sources define near-infrared, mid-infrared, and far-infrared differently, for the purposes of this thesis, these bands will be defined over the

ranges outlined in Table 3. It also includes a description of the peak blackbody temperature of an object in this wavelength range and what astronomers typically seek to observe in the particular band.

Table 3. Infrared Radiation Bands[9]

Spectral Region	Wavelength (microns)	Temperature Range (degrees Kelvin)	Typical Applications
Near-Infrared	(0.7-1) to 5	740 to (3,000-5,200)	Peak emission of M and K type stars
Mid-Infrared	5 to (25-40)	(92.5-140) to 740	Peak Thermal emission of satellites
Far-Infrared	(25-40) to (200-350)	(10.6-18.5) to (92.5-140)	Astronomy viewing of cold objects

Concentrating in the near-infrared (NIR) region, an IR detector looking at the 1-1.5 micron range will need to be able to view a sufficient number of K and/or M type spectral class stars which will be discussed later in the background section. In addition to the defined IR radiation bands, astronomers have developed specialized IR bands to take into consideration opening through the atmosphere. Table 4 outlines these infrared windows.

Table 4. Infrared Windows in the Atmosphere[10]

Wavelength Range	Band	Sky Transparency	Sky Brightness
1.1 - 1.4 microns	J	high	low at night
1.5 - 1.8 microns	H	high	very low
2.0 - 2.4 microns	K	high	very low
3.0 - 4.0 microns	L	3.0 - 3.5 microns: fair 3.5 - 4.0 microns: high	low
4.6 - 5.0 microns	M	low	high
7.5 - 14.5 microns	N	8 - 9 microns and 10 -12 microns: fair others: low	very high
17 - 40 microns	17 - 25 microns: Q 28 - 40 microns: Z	very low	very high
330 - 370 microns		very low	low

Discussions of the LEO Raven experiments will explore values in the J and H bands later in this research thesis. The LEO Raven research will observe radiation incident from both stars and reflected radiation from satellites, and radiation from the satellite will be characterized by the spectral class of the Sun since this radiation is being reflected to Earth by the observed satellite. For further reading about infrared electromagnetic radiation see *The Infrared Handbook* edited by William L. Wolfe and George J. Zissis. Section 2.2 discusses aspects of reflection, and section 2.3 explores various star properties.

2.2 Reflection

Conducting research and designing remote sensing systems in the IR region presents two distinct advantages: 1) The radiation source or sun (for reflected radiation) is most intense in the visible which carries over to a strong infrared reflection and 2) good commercially available near infrared detectors exist which lowers the cost of a collection system. The reflected signal depends upon the composition and shape of the object. With regards to satellites, solar panels, surface roughness, and the sharper metal edges of a satellite create ideal objects for solar reflection and detection during daylight. In addition, radiometric factors (detector geometry) define how much of the reflected radiation reaches the detector. Radiometric aspects will be discussed in section 2.4. Figure 3 illustrates how reflected solar radiation changes and reflects off a surface (in this case the ground).

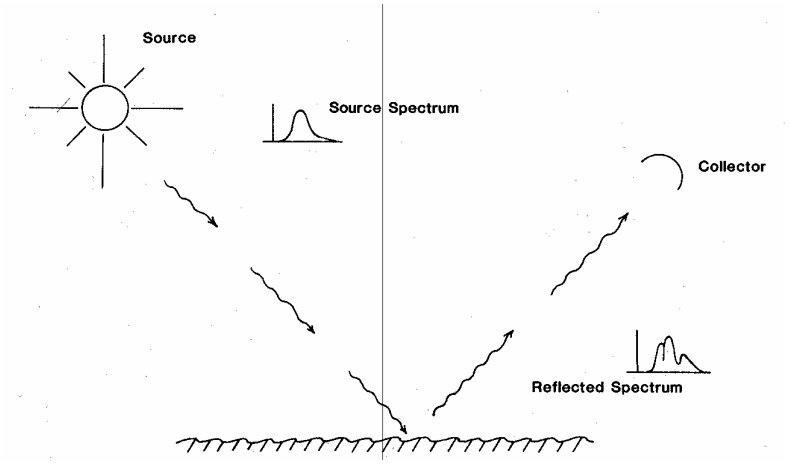

Figure 3. Reflected Radiation[11]

A material's surface albedo is defined as the intensity reflected from the surface divided by the intensity incident on the surface. For a LEO satellite at the top of Earth's atmosphere, the irradiance from the sun ranges from 1350-1480 watts per meter squared. This energy will be reflected with the potential to be detected on Earth's surface. In addition, these reflections can be either diffuse or specular due to the materials surface properties. Kirchoff's Law dealing with absorbance and reflectance explains how much radiation will ultimately be reflected to Earth. Essentially this law states that a portion of the incident radiation will be absorbed by the surface and the rest will be reflected. For a given satellite observation, this absorption loss must be considered since it will reduce the amount of photons incident on the detector. In Figure 4, the spectral radiance of reflected versus emitted radiation is graphed versus the wavelength for a given reflectance (?) and emissivity/absorption (e). Notice that the sun's reflected radiation dominates in the 1-1.68 micrometer range.

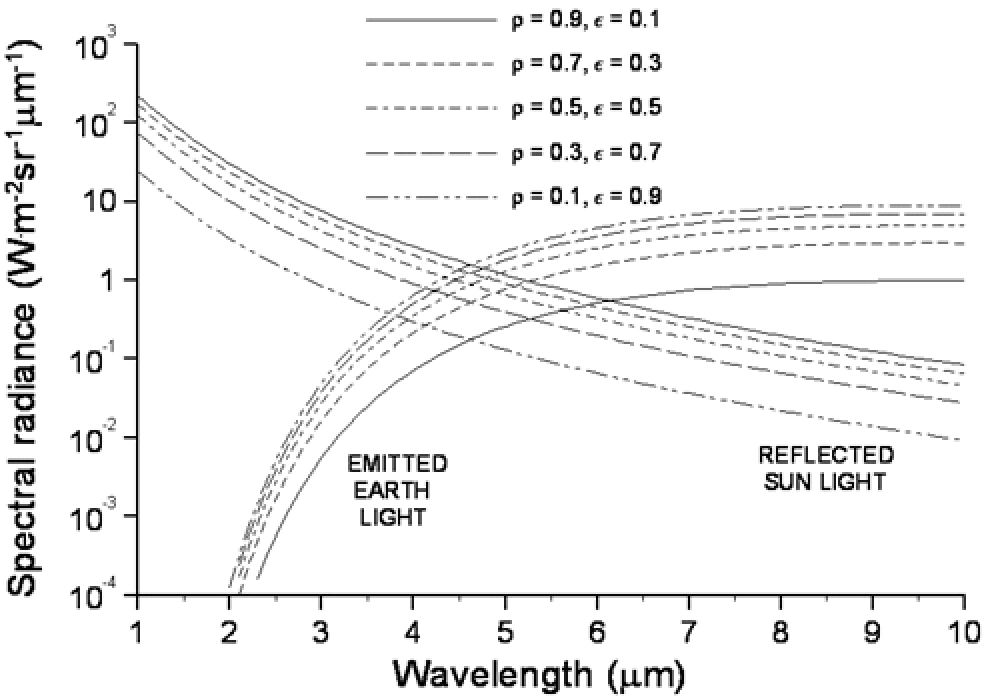

Figure 4. Intensity of Reflected Sunlight[8]

When observing a source for remote sensing purposes, it is necessary to take the spectral characteristics of sources, detectors, optical systems, filters, and the like into account. This is done by integrating the particular radiation product function over an appropriate wavelength interval. Elements of this integration include Planck's Law, Stefan-Boltzmann Law, and Wien's Law.

Planck's Law describes the spectral radiant emittance of a perfect blackbody as a function of its temperature and the wavelength of the emitted radiation. The spectral radiance can be found by dividing p(?,T), the radiation emitted as a function of wavelength and temperature, by p.[8] Below p(?,T) is represented as:

$$r(l,T) = \left(\frac{8phc}{l^5}\right)\left(e^{\frac{hc}{lk_BT}} - 1\right)^{-1}$$

(1)

This equation and the Stefan-Boltzmann law will be used to describe the radiation incident on a detector from a star or reflected from a satellite. Stefan-Boltzmann's law deals with the integration of the Planck function which in turn obtains the total radiation at all wavelengths. The total power radiated from a blackbody varies as the fourth power of the absolute temperature.

$$\int_0^\infty r(\lambda)d\lambda = \left(\frac{8\pi^5 k_B^4}{15c^3h^3}\right)T^4 = \left(\frac{c}{4}\right)\sigma_{SB}T^4 = \frac{Total\ Enenrgy}{Volume} \qquad (2)$$

Wien's displacement law gives the wavelength for maximum radiation emitted. The higher the temperature the shorter the wavelength at which the peak occurs. The sun has a temperature of 5900 Kelvin which results in a peak wavelength at 0.491 microns in the blue region of visible light.

$$\lambda_m T = 2.898 x 10^{-3} Km \qquad (3)$$

Total emissivity of a body is the ratio of its total radiant emittance to that of a perfect blackbody at the same temperature. Thus, emissivity is a measure of the radiation and absorption efficiency of a body. It is a function of wavelength and will usually increases with temperature. Radiation incident on a substance can be transmitted, reflected (or scattered), or absorbed.[12] Due to these radiation losses, a satellite acts as an imperfect blackbody or gray body. The radiation reflected to the detector will not be what initially reached the satellite and

will need to be considered in the magnitude calculations of a satellite. As for stars, the radiation from them passes directly into the atmosphere. See chapters 1-3 of *Infrared Technology Fundamentals* by Monroe Schlessinger for more information on reflection and infrared proprieties. Section 2.3 introduces star properties relevant to this research.

2.3 Star Properties

Stars emit radiation across the entire electromagnetic spectrum, and IR radiation can reveal information above and beyond just visible light. Stars are grouped into categories by size, luminosity, and density.[13] Spectral classification stacks stars in order of decreasing temperature which can be found using Wien's displacement law Equation (3). Table 5 illustrates a Georgia State University categorization of the established star spectral classes.

Table 5. Star Classes[14]

Star Class	Temperature (degrees Kelvin)	Star Color
O	30,000-60,000	Blue stars
B	10,000-30,000	Blue-white stars
A	7,500-10,000	White stars
F	6,000-7,500	Yellow-white stars
G	5,000-6,000	Yellow stars (like the Sun)
K	3,500-5,000	Yellow-Orange stars
M	< 3,5000	Red stars

Astronomers use infrared sensors to observe the stars, and to better categorize stars, a magnitude scale has been developed. This scale includes both the apparent and absolute magnitude of the star. Apparent magnitude is how bright a star appears from the Earth.

Absolute magnitude reflects a stars' brightness as compared to every other star.[15] Many things can influence how bright a star looks: (1) How much energy the star is giving out, in joules/sec or watts; (2) How far away the star is from the observer; (3) How much interstellar dust is blocking the star's light; (4) How much air from Earth is blocking the star's light (called atmospheric extinction). In practice, the Earth's atmosphere will make a star look about 0.5 magnitude fainter, and this varies with the altitude of the star above the horizon. We can account for this because we know what our air is like. We can even account for the atmospheric extinction as a function of the wavelength of the light -- the dimming of light by our atmosphere isn't the same for all colors. Interstellar dust makes a star look redder than its usual spectrum, and there are ways to account for this, too.[15]

The following table demonstrates how brightness changes as a star moves on the magnitude scale. Note that brighter stars have a smaller magnitude. The modern magnitude scale is a quantitative measurement of flux of light coming in from a star, and the scale is logarithmic. The equations for the apparent and absolute magnitude calculations are below: (Note that I is the radiant flux, m is apparent magnitude, M is absolute magnitude, and d is distance.)

$$m = m_o - 2.5\log(I / I_o) \quad (4)$$

$$M = m + 5 - 5 * \log d \quad (5)$$

Table 6. Star Magnitude vs. Brightness

Magnitude Difference	Brightness Difference
0.0	1.0
1.0	2.512
2.0	6.310
3.0	15.85
4.0	39.81
5.0	100.0
6.0	251.2
7.0	631.0
8.0	1585
9.0	3981
10.0	10,000

Figure 5 depicts the Big Dipper which gives a common benchmark for typical star magnitudes:

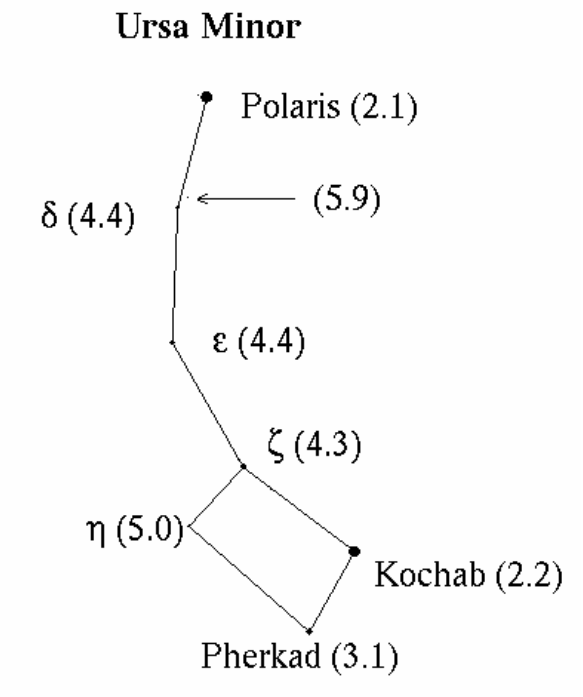

Figure 5. Typical Star Magnitudes

For a more information relating to star properties, see *Allen's Astrophysical Quantities*, 4th Ed. by Arthur N. Cox. The following section will deal with the transmission of radiation from a given source (either star or satellite) and discuss how much of the energy will get to the IR detector.

2.4 Radiometry

Radiometry deals with radiant energy of any wavelength. Photometry, on the other hand, deals with only the visible portion of the spectrum. Variations in radiometry include spectral emission, transmission of the atmosphere and optics with wavelength, and differences in detector and film response with wavelength. Intensity drops off as a function of the one divided by the squared distance the observer is away from the source.[12]

Table 7. Radiometric Terminology

Term	Description	Units
Irradiance (H)	Power per unit area incident on a surface	Watts m^{-2}
Radiance (N)	Power per unit solid angle per unit area from a source	W $ster^{-1}$ m^{-2}
Radiant Intensity (J)	Power per unit solid angle from a source	W/ster
Radiant Power/Flux (P)	Rate of transfer of energy	Watts or J/s
Radiant Energy (U)	Energy	J
Radiant Emittance (W or M)	Power per unit area emitted from a surface	W/m^{-2}

Key points relating to radiometry include: (1) The radiance of a surface is conventionally taken with respect to the area of a surface normal to the direction of radiation; (2) The radiance of a Lambertian surface is constant with respect to theta; and (3) The radiance of the image is equal to that of the object times the transmission of the system.

Laying the foundation for solid angle geometry will aid in radiometric analysis of IR radiation. A detector's geometry in relation to the source of the radiation will be importance for its effectiveness as a collection device. Common terms used with solid angle geometry include the field of regard, everything it is possible to see, and field of view, everything that is being seen by the sensor. Here are definitions of angles used to describe the solid angles:

$$q = \frac{\text{arc length subtended on circle}}{\text{radius of circle}} = \frac{s}{r} \tag{6}$$

$$\Omega = \frac{\text{area on surface of sphere}}{\text{radius of sphere squared}} = \frac{A}{r^2} \tag{7}$$

Figure 6 pictorially represents the solid angle geometry:

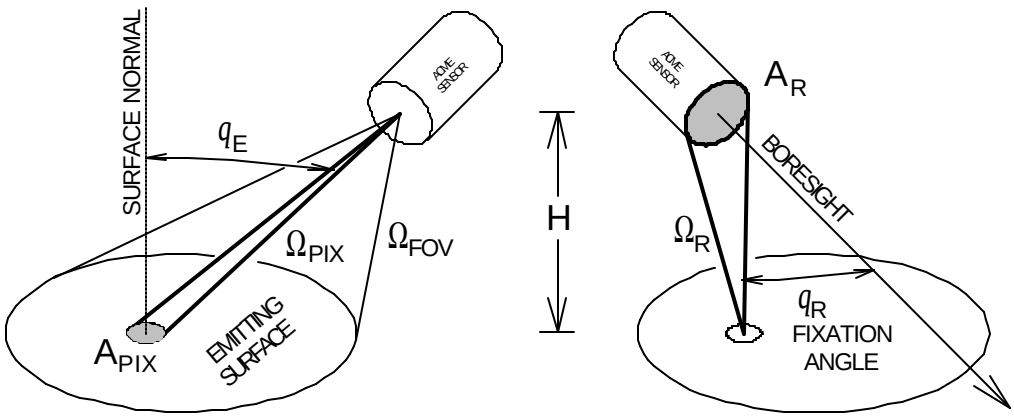

$$\Omega_{PIX} \approx \frac{A_{PIX\perp}}{r^2} = \frac{A_{PIX}\cos q_E}{\left(H/\cos q_E\right)^2} = \frac{A_{PIX}}{H^2}\cos^3 q_E \qquad \Omega_R \approx \frac{A_{R\perp}}{r^2} = \frac{A_R \cos q_R}{r^2}$$

Figure 6. Solid Angle Geometry[8]

This figure effectively explains the amount of radiation which reaches a detector. The first case illustrates an extended source and the second diagram shows a point source. Throughout this research, the point source will effectively explain the reflections off a satellite and radiation incident from a star. Chapter 2 of *Infrared Technology Fundamentals* by Monroe Schlessinger explores infrared radiometry in more depth and can be reference for further reading. Once the solar radiation has been reflected off the satellite and the stellar radiation reaches the Earth, they must both pass through the Earth's atmosphere. The atmosphere greatly effects what radiation can be seen by the detector, especially during daylight. Section 2.5 introduces these atmospheric challenges.

2.5 Atmospheric Challenges

A fundamental challenge for conducting infrared collection from the ground to space occurs when the radiation passes through the Earth's atmosphere. Water, carbon dioxide, and other atmospheric molecules prevent radiation transmission across multiple spectral bands. When designing detectors both for ground facilities looking to space and spacecraft looking to the ground, these limitations must be taken into account. Note that significant "outages" occur in the reflected and thermal IR. In addition, the amount of atmosphere crossed by the radiation and particulates in the air will affect transmission. Figure 7 shows transmission windows through the Earth's atmosphere.

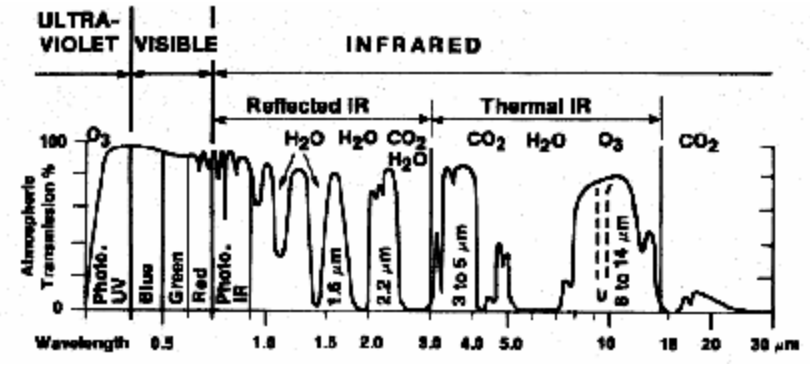

Figure 7. Transmitted Radiation through Earth's Atmosphere[16]

Figure 8 illustrates a blackbody radiation curve of the sun. The sun's peak radiation occurs in the Blue at about 5900 degrees Kelvin. Radiation collected in the reflected IR will be largely influence by the sun, since it is the source of the radiation used in passive collection of

satellite targets. Figure 8 overlays the Earth's atmospheric transmission windows on the solar radiation.

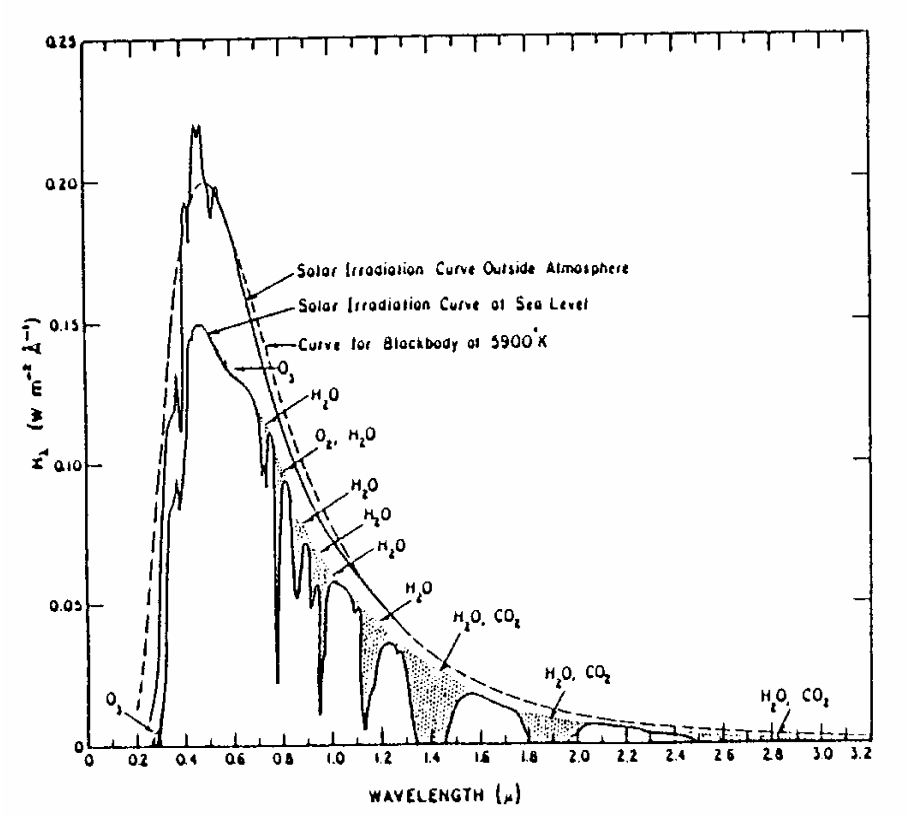

Figure 8. Sun's Blackbody Radiation Transmitted through the Atmosphere[8]

Figure 9 shows the percentage of transmission of a general source through the atmosphere.

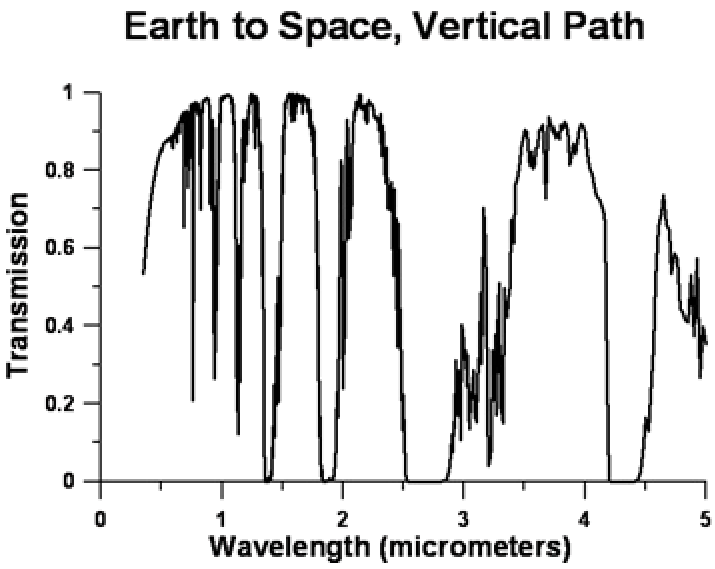

Figure 9. Transmission from the Earth to Space[17]

More information on atmospherics can be found in chapters 4 of *Infrared Technology Fundamentals* by Monroe Schlessinger. Once the radiation, whether reflected from a satellite or incident from a star, passes through the atmosphere, it must also pass through the optics of the telescope and onto the detector. Section 2.6 discusses optics and detectors.

2.6 Optics and Detectors

Optics, like the atmosphere, introduce transmission losses, and the secondary mirror blocks some of the incoming radiation. These issues will be discussed in more depth in section 4.8. Although, the scope of this research will not cover an in depth exploration of optics, but reference *Modern Optical Engineering* by Warren J. Smith for a more detailed discussion issues surrounding optics.

IR detectors are classifieds as either photon detectors or thermal detectors. Photon detectors deal with semiconductor IR detectors where the radiation is absorbed within the material by interaction with electrons.[18] These detectors also show a selective wavelength dependence of the response per unit incident radiation power. They exhibit perfect signal-to-noise performance and a very fast response, but cooling requirements are their main obstacle. The LEO Raven research will focus on a photon detector.

Infrared FPAs are usually classified as monolithic or hybrid. The choice of a FPA will depend on the technical requirements, projected costs, and schedule. Monolithic FPAs utilize some multiplexing in the detector material rather than in an external readout circuit. Its basic element is a metal-insulator-semiconductor (MIS). This MIS capacitor detects and integrates the IR-generated photocurrent. Hybrid FPAs are built with different substrates and mated with each other by the flip-chip bonding or loophole interconnection. These FPAs allow optimization of the detector material and independent multiplexing.[18] The Merlin camera used in this research is a monolithic FPA.

Over the past four decades mercury cadmium telluride (HgCdTe) has become the most prominent semiconductor for the middle and long wavelength (3-30 microns) IR photodetectors. Detectors in the short wavelength IR are dominated by III0V compounds (InGaAs, InAsSb, InGaSb). HgCdTe still maintain a large market share due to its fundamental advantages, flexiblitiy, and ability to cover the whole IR spectral range with nearly the same lattice parameter.[18] Despite HgCdTe's popularity, the Indigo Merlin detector used for the LEO Raven research is an InGaAs detector and reasons for this will be discusses in section 3.1.7.

Figure 10 shows how typical detector materials respond at a given wavelength. The InGaAs detector has been maximized for the near infrared wavelengths needed for the LEO Raven.

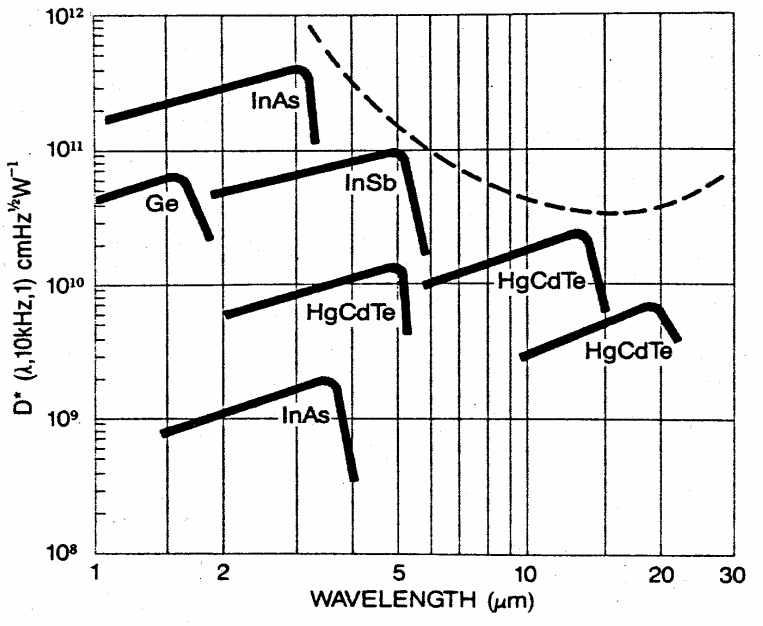

Figure 10. Detector Sensitivity

Figure 11 reveals what a visible image of Orion versus an infrared image of Orion taken from space looks like. Note the increase in observable objects in the IR image.

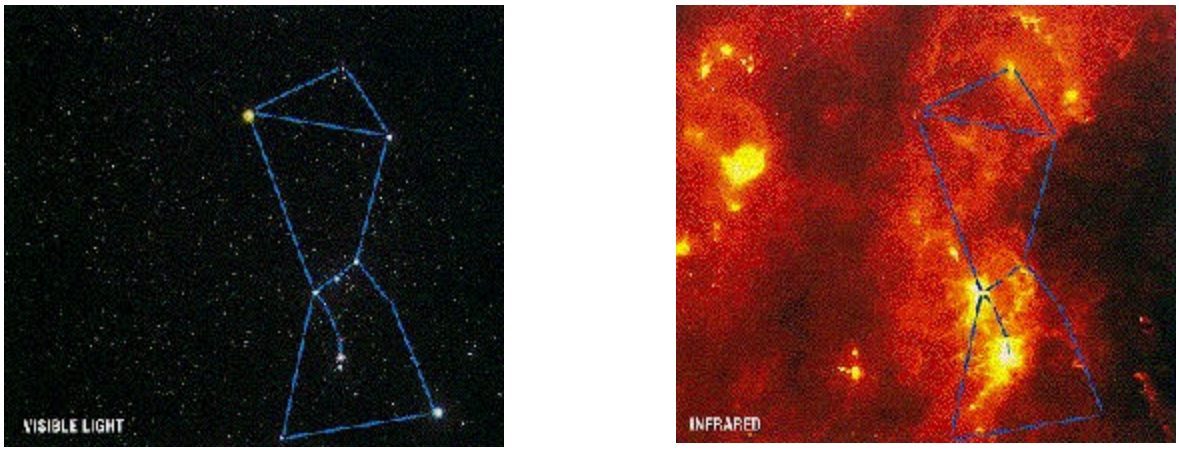

Figure 11. Constellation Orion in visible (a) and infrared (b)

While space-based IR sensing produces excellent results for astronomy, these systems are expensive to develop, launch, and maintain. Many astronomical observations are conducted from ground-based observatories. These systems must deal with the complexities presented by the atmosphere. The best location for IR observatories is in high, dry mountain areas (above much of the water vapor in the atmosphere). At these altitudes astronomers typically study IR wavelengths centered around 1.25, 1.65, 2.2, 3.5, 4.75, 10.5, 19.5 and 35 microns.

When IR wavelengths are collected both the atmosphere's emission and the observed objects emission are collected. The atmospheric emission in the IR must be subtracted to get an accurate measurement. To help mitigate these problems both civilian and military astronomers have developed adaptive optics systems to compensate for the atmosphere. This aids in eliminating distortions, but not water vapor problems.[19] The challenges of the atmosphere and sky background discussed here will be addressed at more length in section 3.1.4 and 3.1.5, but the use of adaptive optics will not be addressed since the goal of this system is a low cost,

commercial LEO Raven. Adaptive optics introduce higher prices and complexity. Combining all of the parts discussed in sections 2.1 to 2.6 results in an end-to-end approach for the space to detector model used for analysis in section 4.8. Section 2.7 summarizes this end-to-end approach in this space to detector model both graphically and mathematically.

2.7 The Master Equation

Combining each of these pieces yields a complete analysis approach. Considering the particular electromagnetic band pass, radiometry, atmospheric transmission, telescope optical properties, and detector parameters yields a final end-to-end approach. Figure 12 shows an excellent summary of the space to detector problems posed to the LEO Raven system.

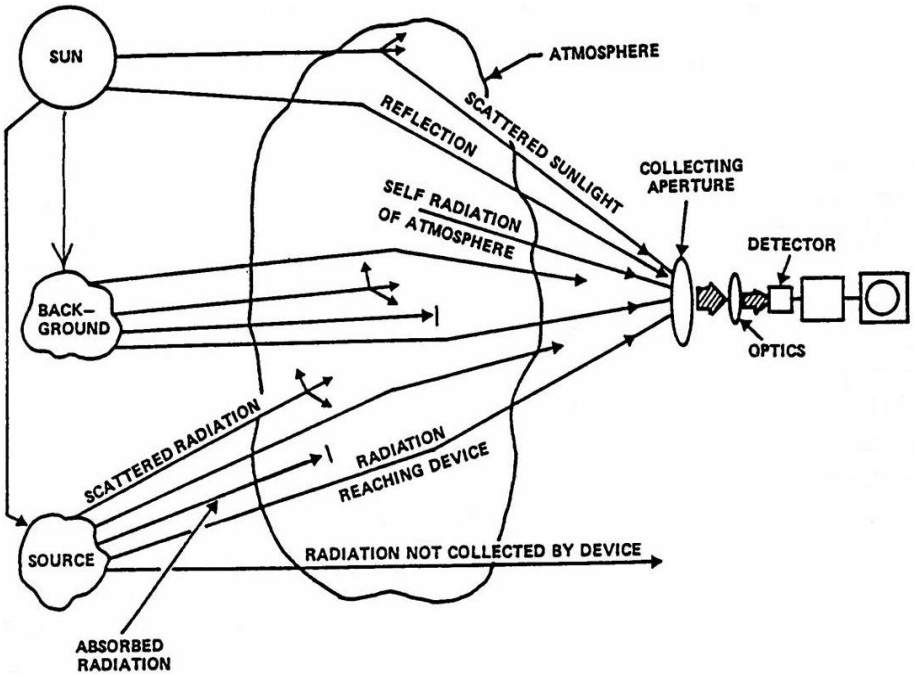

Figure 12. Radiation Collected by a Detector[8]

Integrating these concepts produces a "grand-daddy" type equation to find the final amount of radiation detected.

$$N = \int_{BANDPASS} \left(\frac{I_l}{hc/l} \right) \left(\frac{\cos q_R}{R^2} \right) (t_{ATM})(A_R t_{OPT})(h\ G)\, d\, l\ \Delta t_{INT} \tag{8}$$

where

N = Total count rate

I_λ = Source irradiance

The cosine term accounts for the radiometry of satellite/observer geometry and the distance of the source.

t_{ATM} = Transmission of the radiation through the atmosphere

$A_R t_{OPT}$ = Area of the telescope and optical transmission through the telescope

?G = Quantum Efficiency and Gain of the detector

d? = Band pass of the detector (0.9-1.68 in this research)

? t_{INT} = Integration time of the detector

Analysis using this space to detector equation will be done with data collected on the RME Raven telescope. See section 4.8 for the details. This space to detector model will also serve and the construct for the LEO Raven research methodology outlined in chapter 3.

III. Methodology

Researching the LEO Raven requires collecting data on three telescope systems at the Maui Space Surveillance Site and Remote Maui Experiment (RME) location. These systems include the 0.42m HANDS Raven, 1.60m GEMINI, and the 0.36m RME Raven. Initial experiments focus on the 0.42m HANDS Raven and address the issue: How fast can a typical Raven mount track, and will it be sufficient for LEO satellites? The 1.60m GEMINI data collection will occur during daylight hours and seek to answer the question: How many stars could potentially be seen above the sky background, and can accurate astrometry be done? The third data collection experiments on the 0.36m RME Raven deal with the question: What is the limiting magnitude of the current Merlin-RME Raven configuration, and can it observe LEO satellites during daylight? At the conclusion of these experiments, the questions posed in Table 1 will be answered, and design recommendations will be made for the daylight LEO Raven.

Leading into any research endeavor, modeling of the problem becomes very important. Throughout this research, several software tools and models were incorporated to help explain and check the final research results. Star field densities were found using the 2MASS star catalog of infrared stars. Plexus (MODTRAN) models were utilized to model sky background and atmospheric transmission. In addition, a space to detector model estimates the total power received at the detector which can be compared to observed values. This model can in turn be used to scale results to any proposed daylight LEO Raven system.

3.1 Space to Detector Model

The essence of this research deals with understanding electromagnetic radiation emitted from the sun and other stars and how it interacts with the satellite, atmosphere, telescope optics, and detector. Observing methods utilize passive imaging of the satellite using reflected sunlight. The following subsections for 3.1 describe the space to detector model as it relates to the specific infrared bands, optics, and detector used while researching at MSSS. Specific space to detector models for the 0.36m RME Raven telescope and Indigo Merlin detector (0.9-1.68 micron band pass) setup will be explored in section 4.8.

3.1.1 Electromagnetic Radiation

Electromagnetic radiation emitted from the sun travels to earth and eventually comes into contact with a satellite. The sun's electromagnetic radiation can be modeled using Plank's Law as a blackbody with a peak temperature of 5900 K. This results in a peak wavelength, via Wien's law, in the blue or 0.4 micrometers. Typical exoatmospheric solar irradiance for the sky in the 0.9 to 1.68 micron band can be seen in Figure 13.

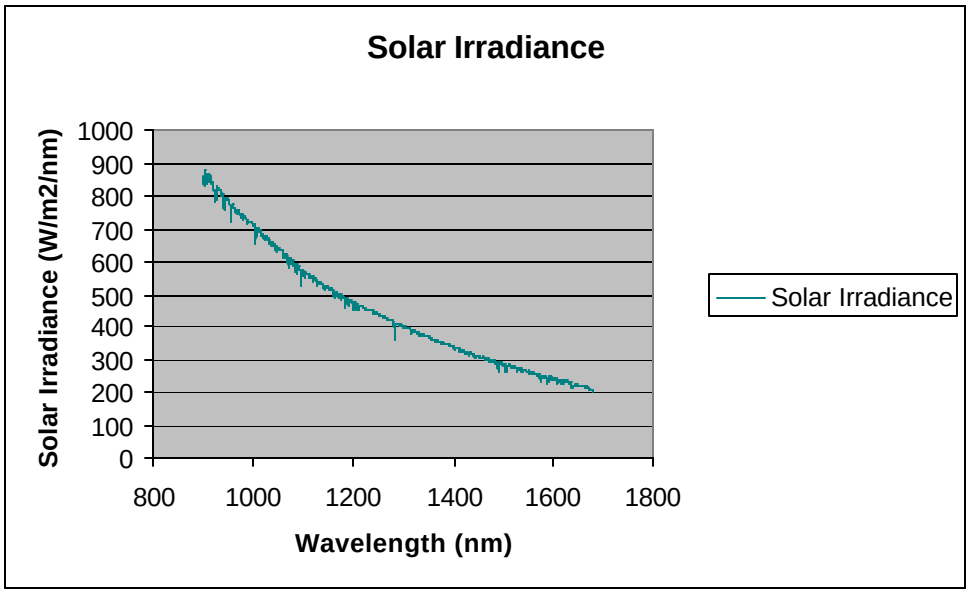

Figure 13. Exoatmospheric Irradiance

This curve represents the solar irradiance before it passes through the atmosphere and does not take into account reflection losses from the satellite. Section 3.1.2 discusses the satellites of interest for the LEO Raven research.

3.1.2 Satellite Targets of Interest

In laying out the test plan for the Daytime LEO Astrometry research, satellite targets needed to be selected. For an in depth description of astrodynamics and orbits see *Understanding Space* by Jerry Sellers.[30] Laser ranged satellites with accurately known reference orbits were chosen. This will allow a comparison of the observed data, which will produce a predicted orbit through astrometry, to the known truth orbits of the "calibration" satellites. In addition, these satellites needed to be in LEO and have a magnitude greater than

8-9 in order to be seen by the DAS sensor. These were the calibration satellite numbers as provided by Dr. Chris Sabol: 8820, 16908, 22076, 22195, 22824, 23560, 25157, 25398, 26977, and 27005.

Table 8. Satellite Laser Ranged (SLR) Targets

Satellite Number	Name	Estimated Magnitude
8820	Lageos	
16908	Ajisiai (EGP)	6.7-8.4
22076	Topex	6.0-7.2
22195	Lagoes II	
22824	Stella	
23560	ERS-2	5.0-6.1
25157	GFO	6
25398	Westpac	9
26977	Cosmos	
27005	Reflector	

Once the targets of interest were chosen a software tool was utilized in order to calculate the predicted rise, culmination, and set times for a particular pass on any given day. PlanPass, a government program developed by Capt Dan Gisselquist, became the standard orbit prediction software. Inputs to PlanPass required to propagate these predictions include weekly and sometimes daily element set updates from AFSPC, the geographic coordinates of the observation location, and the specific satellites of interest.

For purposes of this research, the observations will be conducted in rate track mode versus sidereal and/or stare mode. Rate tracking a satellite slews the telescope at the rate of the satellite which causes stars to streak. Sidereal mode keeps the background stationary. The telescope moves to compensate for the rotation of the Earth and stars appear as point sources where satellites appear as a streak. In stare mode GEO satellites appear stationary while stars

and LEO satellites streak. In this case the telescope position is fixed and the stars appear as streaks moving at sidereal rate along the equatorial axis. Figures 14-16 show a representation of these three tracking modes.

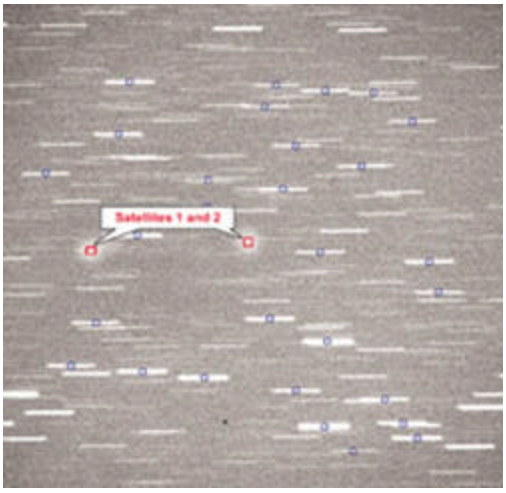

Figure 14. Two satellites detected in stare tracking mode

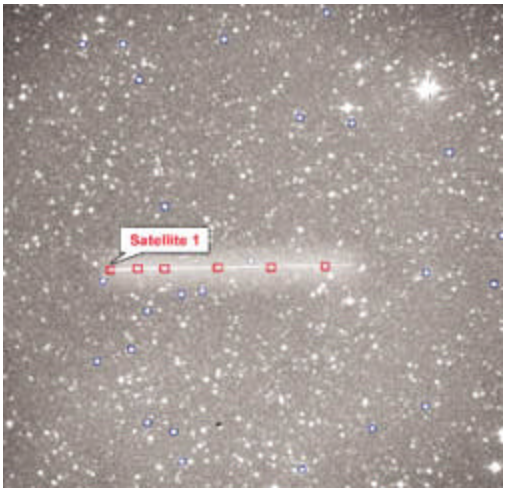

Figure 15. A single satellite detected in sidereal tracking mode

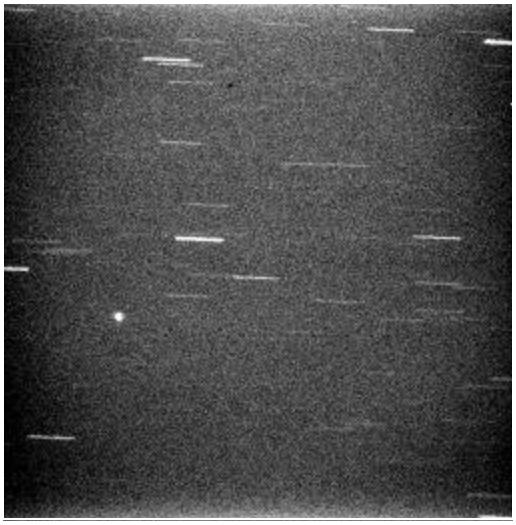

Figure 16. Rate Tracking

Now that target satellites have been chosen, orbit predictions have been made, and tracking method covered, stellar sources must be discussed since they are used in the astrometric process.

3.1.3 Stars

In addition to satellites, this LEO Raven system must be able to see stars in the same field-of-view as the tracked satellite. Just like the sun, other stars also emit electromagnetic radiation which reaches earth. Since the Indigo Merlin collects photons in the 0.9-1.68 micron range, cooler stars will emit more radiation in this band pass. M-type stars exist as the coolest stars with a peak emission around 3000 K or 0.966 microns. Like satellites, all stars will be assumed to be point sources and emit isotropically (independent of direction).

Of the oxygen class stars, K & M types will be the focus. K-type stars are characterized by strong metallic lines and molecular bands which are more pronounced. M-type stars are cool stars with strong neutral metal lines.[13] Typically 70% of the stars in the IR catalogs (used for astrometry) are the cooler spectral types (M, S, and C). In the visible less than 3% of the cataloged stars are these cooler class stars.[13] As a result, sensing in the near-IR band greatly benefits this research and future systems. Now that stellar and reflected satellite radiation has been characterized, both must pass through the atmosphere which will reduce the incident radiation on the detector. Sections 3.1.4 and 3.1.5 explore the atmospheric issues.

3.1.4 Atmospheric Transmission

Before the emitted stellar radiation and reflected solar radiation reach the detector, it must pass through the atmosphere. The atmosphere prevents some of the radiation from reaching earth, scatters some of the radiation, and even causes emission from other molecules. While observing in the NIR helps to avoid daytime atmospheric scattering, specifically Rayleigh scattering effects, atmospheric absorption factors must be considered.[20] In order for the detector to sense any reflected radiation from a target, the signal must also overcome atmospheric scattering and absorption. Within the framework of the specified spectral window, 0.9-1.68 micron range, several IR windows exist. Infrared radiation from stars and satellites passes through with the lowest absorption in the following windows: 0.96-1.12, 1.2-1.3, and 1.5-1.75. Absorption bands which are caused by water vapor exist around these windows

centered at 0.9, 1.1, 1.4, and 1.9.[21] Figure 17 illustrates typical transmission factors in the NIR at a given altitude.

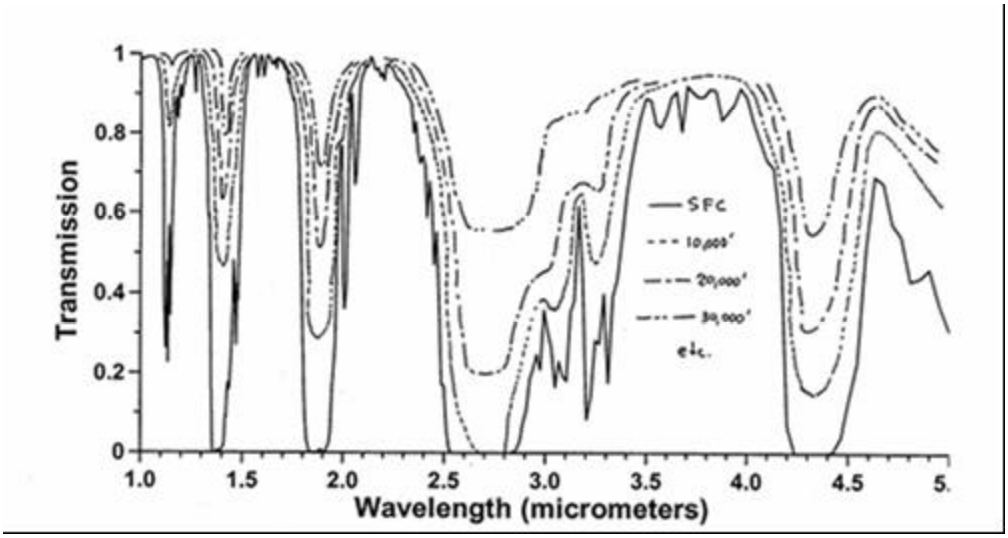

Figure 17. Atmospheric Transmission Based on Altitude

At higher altitudes more radiation reaches the detector due to transmission through less of the atmosphere. The 1.6m GEMINI sits at 10,000' while the 0.36m RME Raven sits at sea level. Each observation point will produce different results. The deployable LEO Raven system cannot assume a higher altitude, so it should be designed for the worst case scenario at sea level. Not only is some of the desired radiation lost due to the atmosphere, radiance and scattering introduce unwanted radiation or noise into the telescope and detector. Section 3.1.5 discusses this added noise.

3.1.5 Atmospheric Radiance and Background

Sky background radiation in the NIR stems from scattering solar radiation and through emission from atmospheric constituents.[21] The scattered solar radiation depends greatly on the corresponding sun angle to the observer's location. Polarization of the sunlight can vary anywhere from 0 to 60% with a maximum at 90 degrees from the sun.[13] In the 0.9-1.68 spectral band pass the thermal emission of the atmosphere, a blackbody temperature of about 300K, induces little effect. In addition, the optics of the telescope emit some optical radiance, but for daytime observation the atmospheric radiance dominates what the detector sees. Typical daytime atmospheric radiance values are 3 W/m^2*sr*micron or over all solar wavelengths on a clear day from 0.1 to 1.15 kW/m^2 (solar and sky irradiance).[13]

Forward scattering in clouds causes another major challenge for observations in the NIR.[13] This also depends on altitude and temperature of the clouds. Reflectance of clouds can exist anywhere from 50 to 90 %. Further information on typical scattering and reflectance values can be found in the IR Handbook. Overall, the irradiance at earth's surface can vary over approximately nine orders of magnitude.[13]

While conducting data collection, several options exist to improve the signal to noise (background) ratio. These techniques include increasing the integration time of the detector, decreasing the FOV, increasing spectral band (or excluding emission bands), and/or moving to a higher altitude. The Indigo Merlin detector used can also be labeled a Background Limited Infrared Photodetector (BLIP) which means that the primary source of noise stems from the background.[8]

Throughout the NIR the daytime sky background worldwide consists of many intrinsically narrow OH emission lines. These hydroxyl lines vary in brightness on a 5-15 minutes timescale. In addition, their amplitude varies 5-10% as atmospheric wave phenomena evolve with the local density of species. Theses emissions occur through a radiative cascade and vary in brightness. As an aside, the strength of OH lines steadily declines after sunset over a period of 60-90 minutes, but for daylight operations their effects will need to be considered.[22] Figure 18 shows OH lines typical for the Hawaiian islands. Details for this data are given below.

- The flux units are given as counts, 1 count = 6 electrons, and are per pixel per 100 seconds.
- The spectra are not corrected for atmospheric transmission.
- Wavelengths are in microns.
- The solid angle for a 0.61" x 0.61" pixel is 8.7455×10^{-12} sr
- The data were obtained by Tom Geballe and Tom Kerr on UT date 1997 19 December.[26]

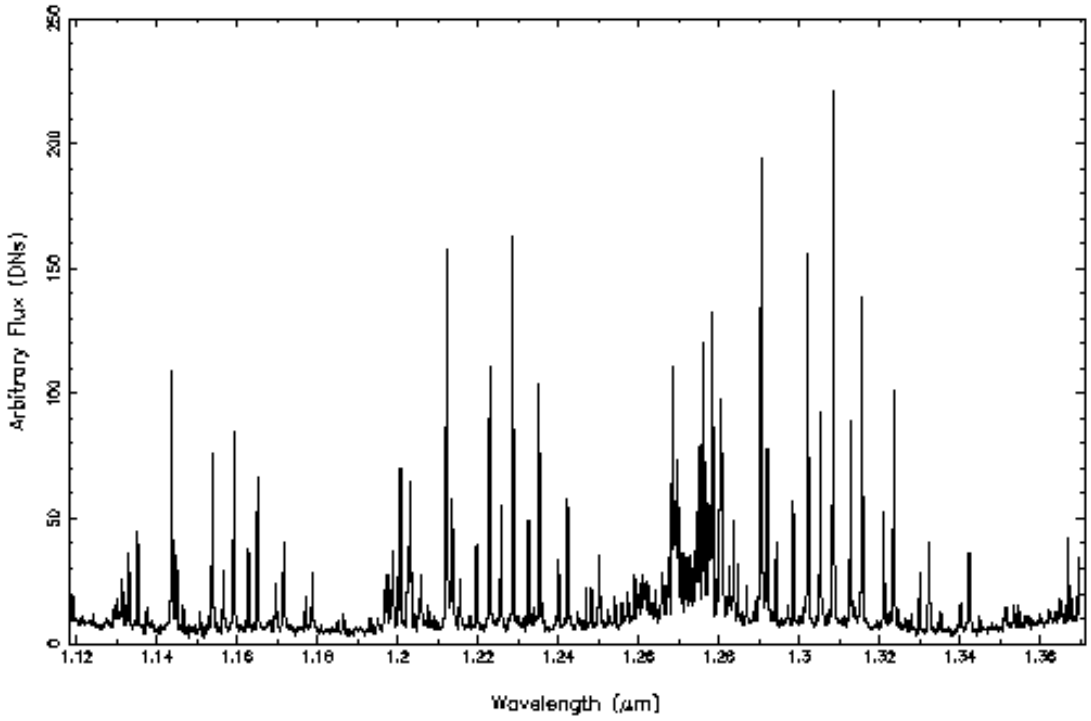

Figure 18. J-Band OH Lines at Mauna Kea[26]

Even though the J-Band only covers a portion of the 0.9-1.68 micron band pass, see how the brightness can vary many magnitudes in a small step in wavelength. With the 0.9-1.68 band pass, these brightness values will introduce more noise into the detector. Reducing the band pass for daylight operations should be considered since other Mauna Kea data shows that brightness peaks from 1.4-1.7 microns. Filtering out the brightness noise in the 1.4-1.7 region will increase the signal to noise ratio and improve the observation platform. Once the incident radiation and sky background reach the detector it must pass through the telescope optics which are discussed in section 3.1.6.

3.1.6 Telescope Optics

Due to the nature of this research, only existing telescopes will be used, but evaluating each setup will provide insight into the development of the LEO Raven. The HANDS Raven addresses mount accuracy. The 1.6m GEMINI explores the ability to do daylight astrometry, but in order to conduct more accurate research for a future LEO Raven system, observing with the 0.36m RME Raven will be important. The RME Raven will best relate to a potential LEO Raven design. As mentioned in section 2.6, optical transmission losses and secondary mirror obscurations will be considered in the radiometric model outlined in section 4.8. Further details of the 0.36m RME Raven, the 0.42m HANDS Raven, and the 1.6m GEMINI telescopes will be discussed in section 3.2. As mentioned earlier, see *Modern Optical Engineering* by Warren J. Smith for a details analysis of optics.[31]

3.1.7 Detector Characteristics

This research utilized the Merlin Camera by Indigo or also called the Daylight Acquisition System (DAS) which is seen in Figure 19. Table 9 shows the Merlin User's guide specifications for this InGaAs detector.

Table 9. Merlin Detector Characteristics[24]

Indigo camera:	320x256 pixel array, 30-micron pixels
Dynamic range:	12-bits, 4096 max counts
Spectral Response:	0.9 – 1.68 microns
Thermo-elec cooled:	291K
Frame rate:	16 – 60 Hz
Exposure time:	10usec to 16msec
Gain setting 0:	0.17 uV/e-
Full-well:	18x10^6 e-

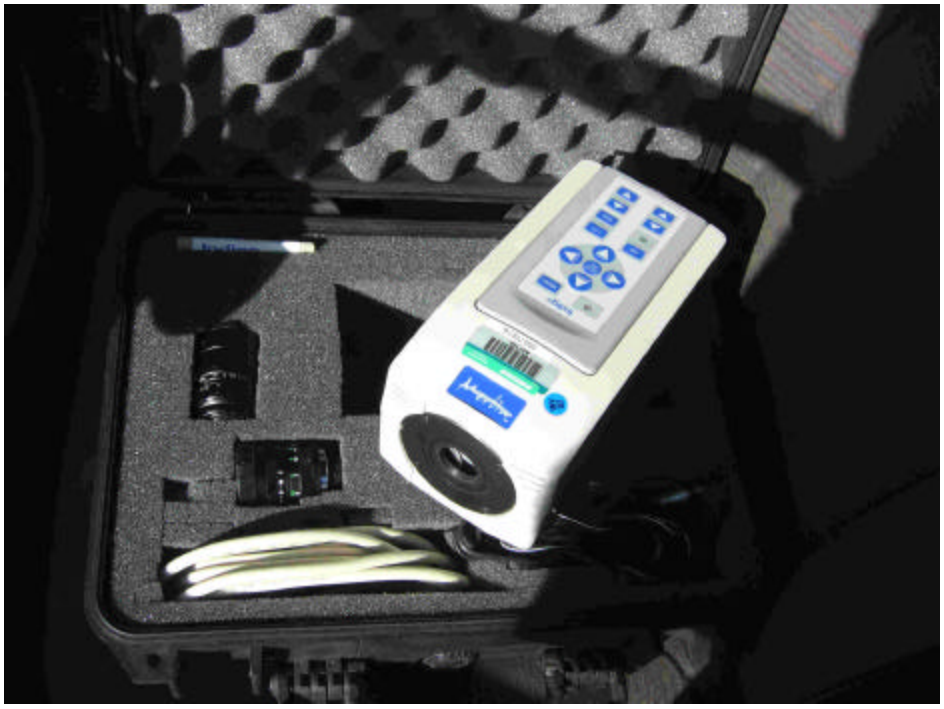

Figure 19. DAS-Merlin Camera

The Merlin camera's photo-responsivity and quantum efficiency can be seen in Figure 20.

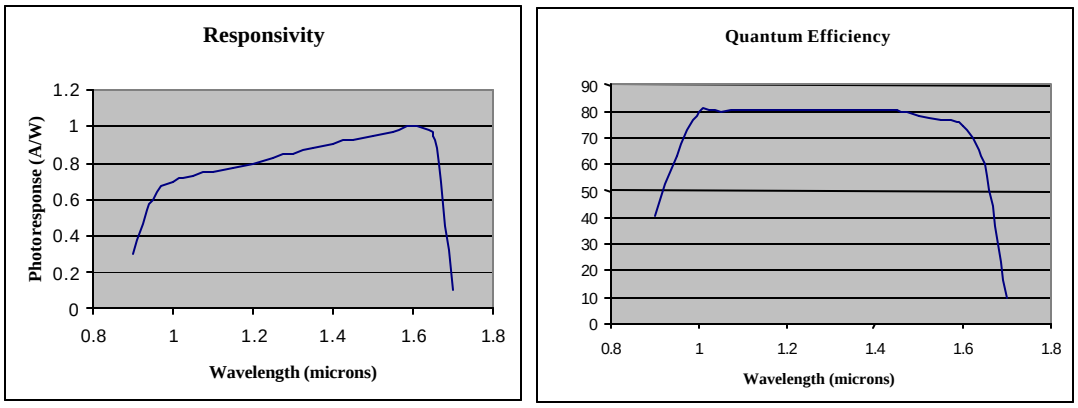

Figure 20. Merlin Responsivity and Merlin Quantum Efficiency[25]

Observations occurred with this camera for several reasons. First of all, this was the near infrared camera available at MSSS and provided the necessary observing capability for initial design studies. Second, the InGaAs technology used by the Merlin is a common commercially available detector. Using a camera of this nature would not require special cooling and would be less expensive. Finally, the InGaAs material is an overall excellent choice. Other commercially available detectors incorporate HgCdTe material, but this would shift the observation windows of the LEO Raven to the 2-5 micron or 5-20 micron range. A detector of this type would introduce several new problems; the sun's blackbody curve drops off more compared to the 0.9-1.68 micron range, a large atmospheric absorption band exists at 2.5-3.5 which further decreases the incident radiation, and finally the 5-20 micron band (thermal infrared) would require a cooling mechanism for the detector to work efficiently. On the contrary, designing a system in the thermal infrared would capitalize on a satellites peak emission in the 8-12 micron band while not being affected by as much of the sky background. However,

as mentioned the cost of cooling the system would add cost to the LEO Raven. Once chosen, the question of stellar viewing became and issue. Can enough stars been seen in the 0.9-1.68 micron band pass? Section 3.1.8 outlines the initial approach to answering this question.

3.1.8 Star Catalog

Before delving too far into the actual research, a guide star catalog extraction must be done in order to determine the stars available to conduct astrometry on the observed objects. If a sufficient amount of stars did not appear in the 0.9-1.68 micron band pass, then conducting daylight, astrometry experiments with the Merlin detector would be a lost cause from the start. One of the most comprehensive and widely used infrared star catalogs is the 2MASS data base. The 2MASS infrared sky survey utilized two 1.3m telescopes based at Mt Hopkins, AZ and Cerro, Chile. Each system used a three-channel HgCdTe detector array (256x256). The channels consisted of a J (1.24 micron), H (1.66 micron), and Ks (2.16 micron) band recorded simultaneously. Observations began in June of 1997 and concluded February 2001 mapping 99.998% of the sky. The 2MASS All-Sky Data Release contains positions and photometry for 470,992,970 objects.[27]

Using this catalog, a filtering routine was applied to the online extraction tool in order to find stars detectable by the Daylight Acquisition System (DAS) used for 1.6m GEMINI and 0.36m RME Raven observations. The filter looked for objects in the H band less than or equal to 9.0 magnitude stars, since that is the limiting magnitude of the DAS on the 1.6m GEMINI. The resulting search yielded a 241 MByte catalog of 1.1million stars. With this many stars

available in the 0.9-1.68 micron band pass, observing stars and a satellite will produce enough data for astrometry on the satellite. Now that enough stars brighter than 9th magnitude ensure observation potential, an overview of the existing data collection hardware in section 3.2 lays the groundwork for the LEO Raven experiments to follow.

3.2 Data Collection Hardware

Initial experiments utilized the 0.42m HANDS Raven telescope which is located in Kihei, HI at the RME facility. This latest generation of Raven telescopes utilizes a Paramount MME German-equatorial mount developed by Software Bisque. Software Bisque has long been a supplier of hardware and software to Raven. In addition to the mount, Software Bisque's The Sky software package controls the mount. Modifications to The Sky, sponsored by the Air Force Research Laboratory, allow for rate tracking of satellites based on standard Two-Line-Element sets (TLE's). While this has been successfully used for deep space satellites for over two years, it had never been tested for LEO objects. The telescope and dome can be seen in Figure 21.

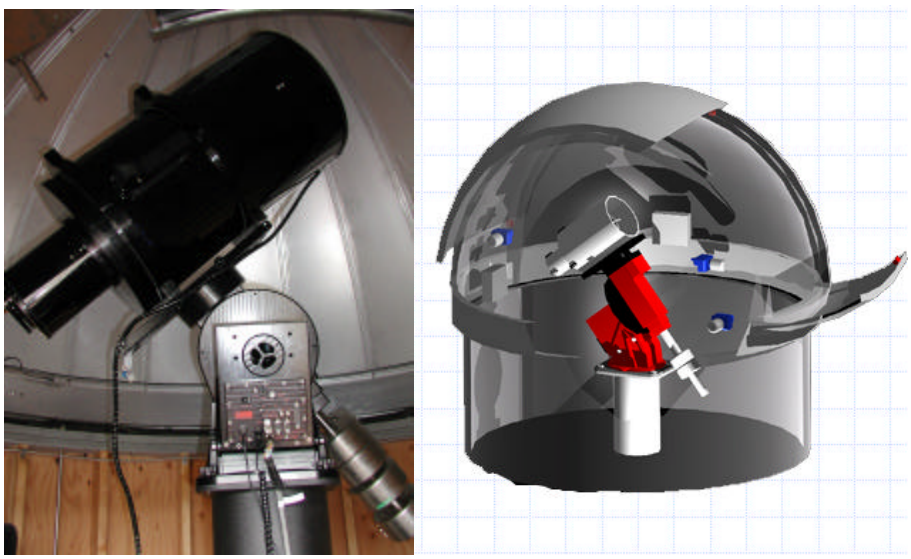

Figure 21. 0.42m HANDS Raven

The Daylight Acquisition Sensor (DAS) sits atop the Maui Space Surveillance Site's (MSSS's) 1.6m telescope near the 10,000 ft summit of Haleakala. Figure 22 shows the 1.6m telescope. DAS is based on a 22" aperture classical Cassegrain telescope with a tertiary fold flat. The telescope has an effective focal length of approximately 180" and is f/8. Since this sensor is used for object acquisition, the DAS sensor field of view is set at 0.5 deg to provide telescope operators with a useful acquisition image size. MSSS experience has shown that this field of view provides enough angular extent to locate most objects within the levels of error encountered in tracking data and pointing drift.[6] This acquisition setup for the 1.6m GEMINI is referred to as the AMOS Acquisition Telescope System or AATS.

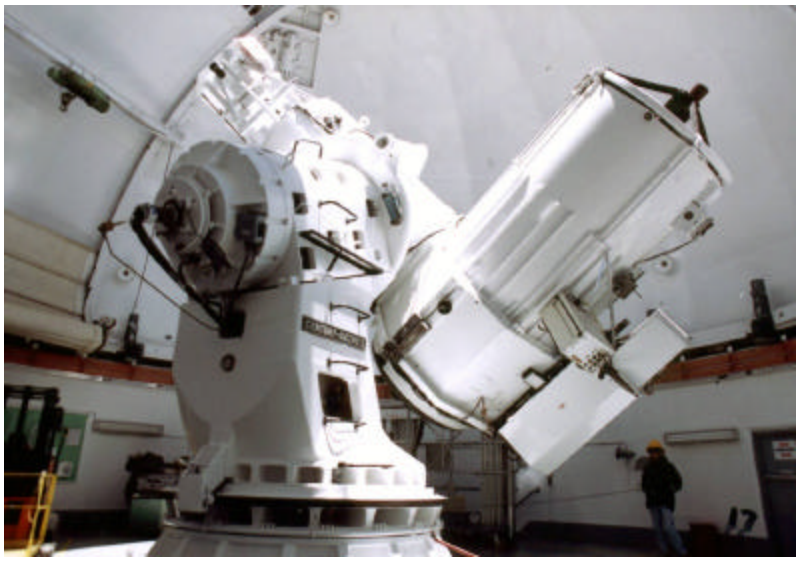

Figure 22. 1.6m GEMINI Telescope

Figures 23-25 show the 1.6m telescope and AATS sensor as viewed looking down into the telescope from the front, the mechanical and optical cross section of the AATS/DAS, and the incoming rays from the telescope.[20] This configuration consists of the DAS/Merlin camera (shown in gray) and optics package piggy backed to the AATS visible imaging sensor compartment.[20]

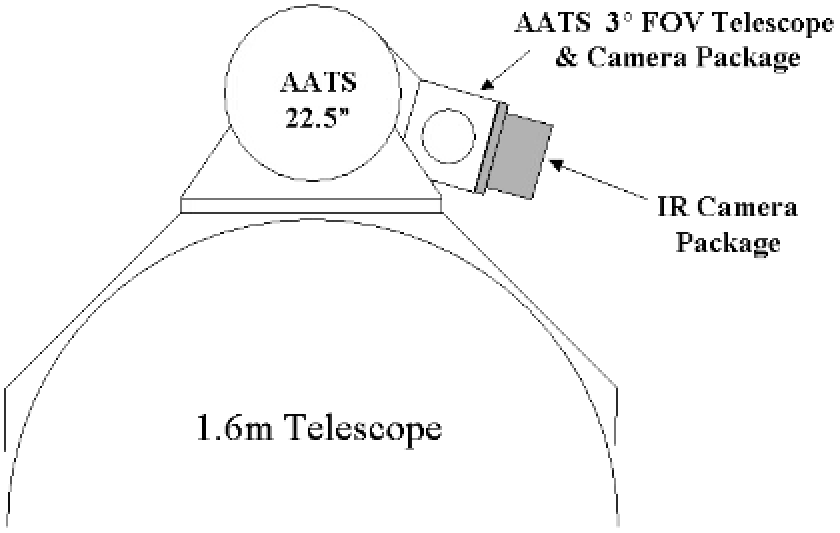

Figure 23. 1.6m Telescope shown with Existing AATS sensor and NIR camera

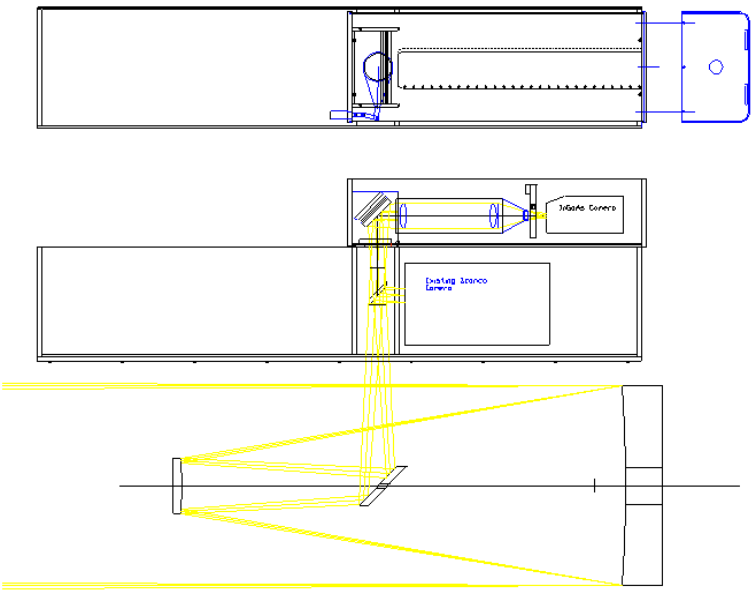

Figure 24. Mechanical and Optical Cross-Section of the AATS/DAS Subsystem

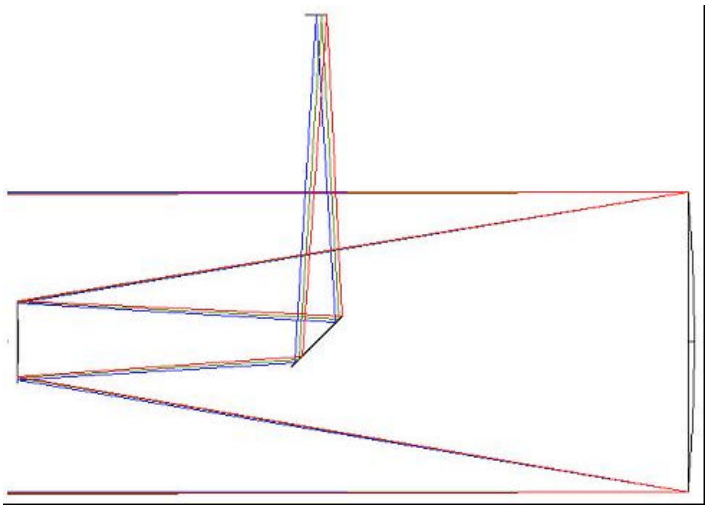

Figure 25. Telescope Showing Incoming Rays From 0, 0.125, and 0.25 Degrees

The Remote Maui Experiment Raven telescope is a 0.3625m, f/3 Torus Optics Newtonian telescope with an open framed truss on a German equatorial mount. The mount tracks objects at rates up to 45 arcsecond/second. The RME Raven dome is made by Ash and is approximately 10 feet in diameter. Figure 26 shows the RME Raven Dome and optical path of the telescope.

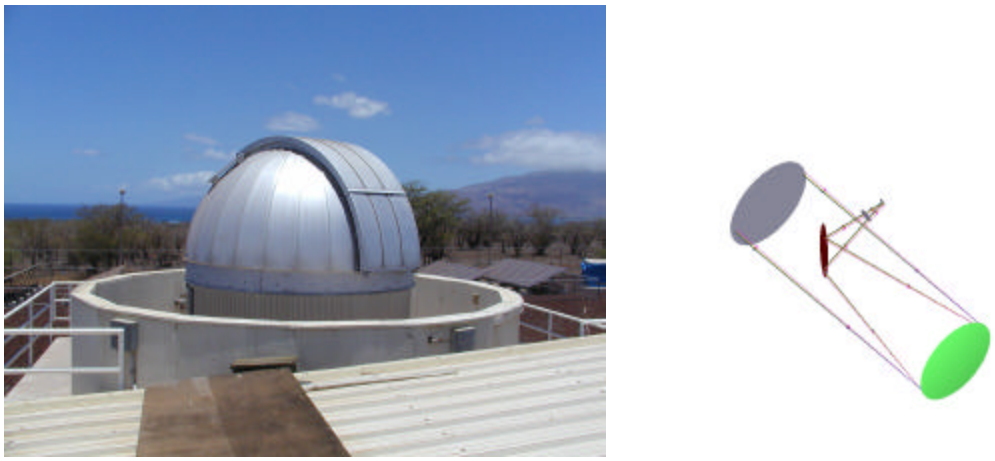

Figure 26. RME Raven Dome and Telescope

Figure 27 shows the interconnection between the five major components of the current Raven setup. The future LEO Raven will incorporate a similar low-cost, commercial setup.

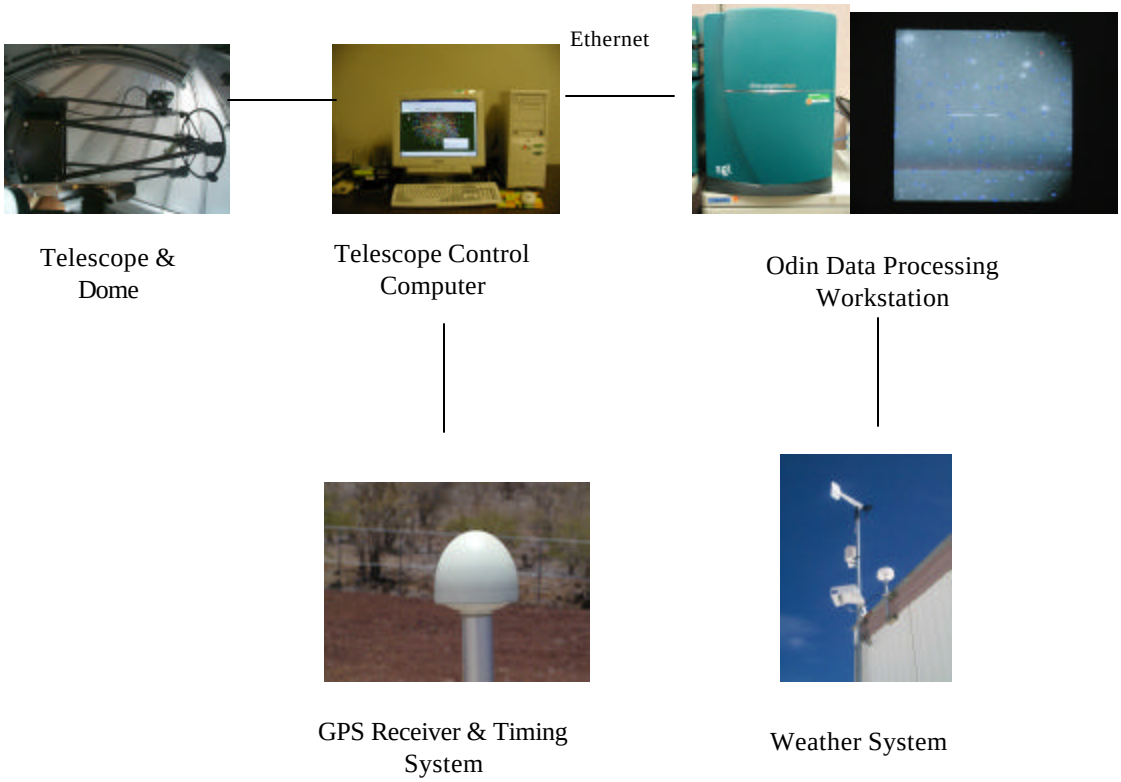

Figure 27: Overview of a typical raven system[2]

Throughout these experiments the 1.6m GEMINI and the 0.36m RME Raven were used to a greater extent, but each set-up provided a test bed for answering a specific question. In addition to the hardware, section 3.3 outlines various software tools used in the research.

3.3 Software Tools

As with most research and development, different software platforms became important to the development of a future LEO Raven system. Software packages were used for mission planning, camera control, telescope mount control, and data analysis. Initial orbit passes for all observations were run using PlanPass. This software inputs orbital element sets from AF Space Command, current geographic position, and the desired target satellites. The output consists of satellite pass horizon break, culmination, horizon set, direction through the overhead sky, and range. Table 10 describes the outputted fields in detail.

Table 10. PlanPass Outputs

Name	Description
SON	Space Object Number
Rise Date	Date when satellite rises above the specified minimum elevation
Rise Time	Fraction of day when satellite rises above the specified minimum elevation
Culmination Date	Date when satellite reaches its maximum elevation in a pass
Culmination Time	Fraction of day when satellite reaches its maximum elevation in a pass
Set Date	Date when satellite sets below the specified minimum elevation
Set Time	Fraction of day when satellite sets below the specified minimum elevation
Maximum Elevation	The maximum elevation angle achieved in a pass
Minimum Range	The minimum range achieved in a pass
Rise Illumination	The illumination condition when the satellite rises above the specified minimum elevation
Culmination Illumination	The illumination condition when the satellite reaches its maximum elevation in a pass
Set Illumination	The illumination condition when the satellite sets below the specified minimum elevation
Rise Azimuth	The azimuth when the satellite rises above the specified minimum elevation
Culmination Azimuth	The azimuth when the satellite reaches its maximum elevation in a pass

Set Azimuth	The azimuth when the satellite sets below the specified minimum elevation
Minimum Nadir Angle	The minimum nadir angle achieved in a pass

The telescope and camera control software is a commercial package called TheSky, developed by Software Bisque. TheSky package consists of several inter-communicating modules, which include

- TheSky application, monitoring the telescope and dome positions,
- CCDSoft providing CCD camera control, including thermoelectric cooling and CCD exposure time,
- Automadome, interfacing to the dome control system,
- GPStfp, interfacing to the Datum GPS receiver,
- Tpoint, providing telescope mount modeling for accurate pointing, and
- Orchestrate, enabling scripting of telescope pointing, satellite tracking, camera acquisition, and data transfer.[1]

Figure 28 provides an image of TheSky software.

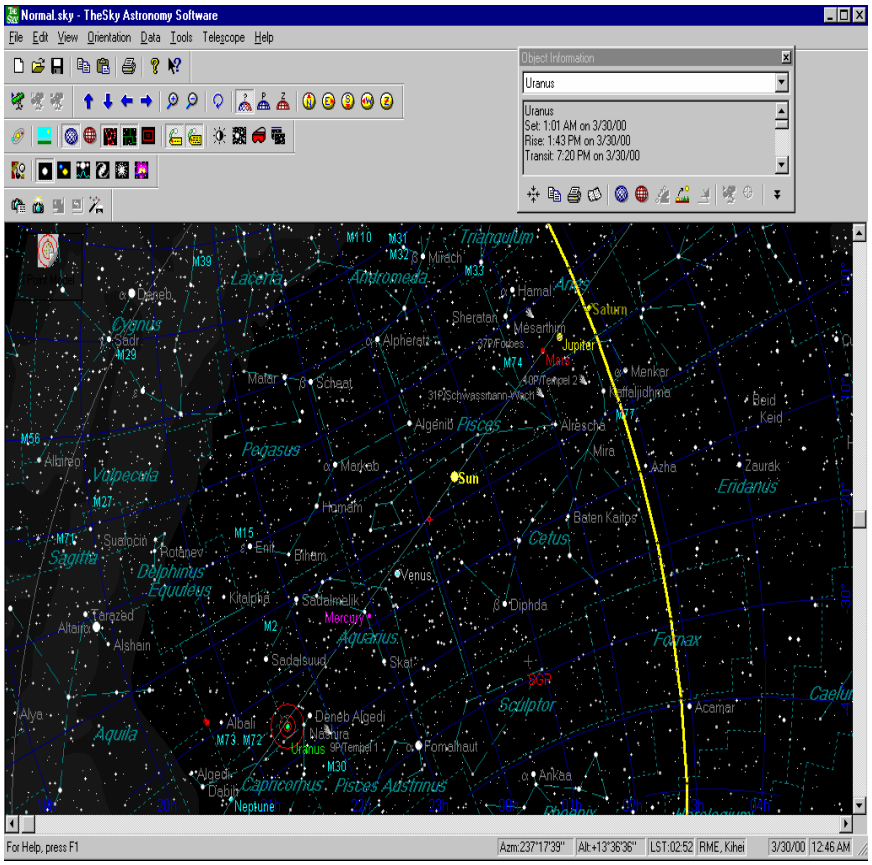

Figure 28. The Sky Software

UltraTalon and IR Vista Software allowed for data collection on the 1.6m GEMINI/DAS setup and the RME Raven/DAS setup respectively. Understanding this software took time, but each piece greatly enhanced collection capabilities. Figure 29 displays an IR Vista screen capture of a star observation encompassing two stars.

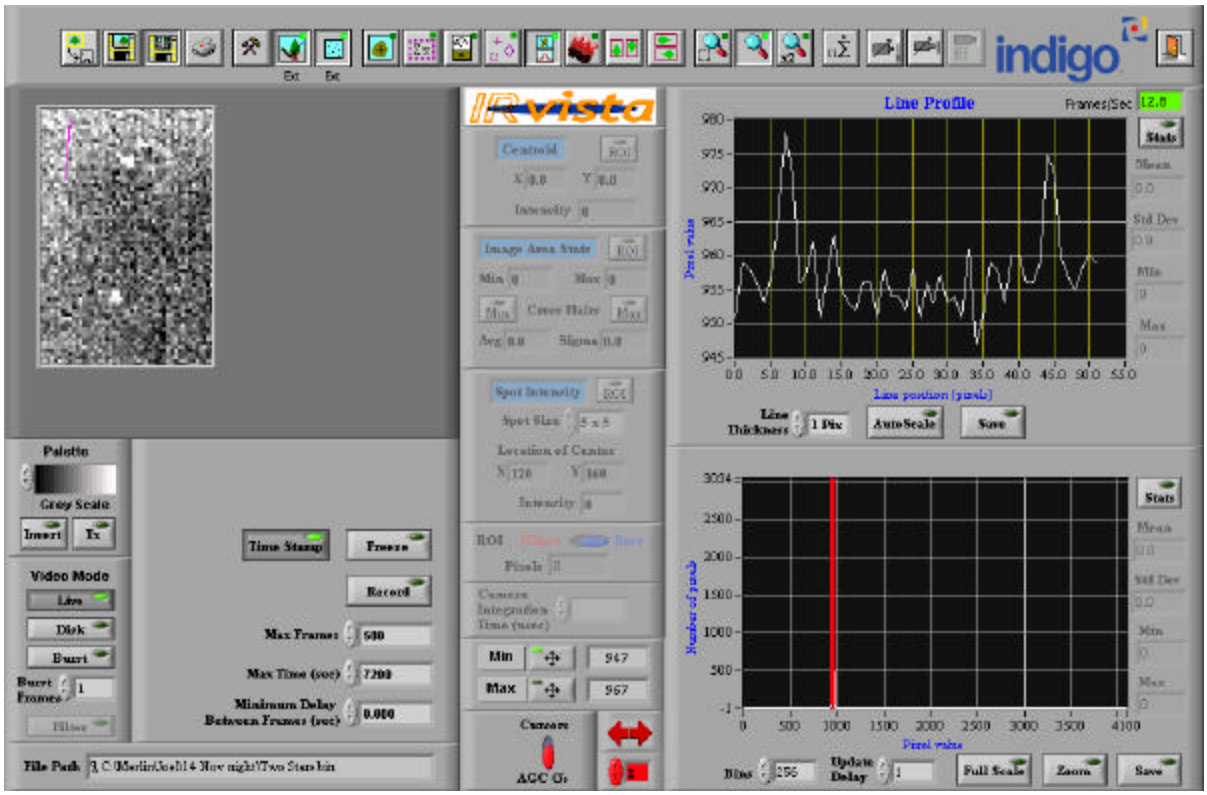

Figure 29. IR Vista

The key to the LEO Raven system is the use of astrometric techniques for position and brightness data. Recall that astrometry compares a satellite to the star background within the sensor field of view; since the position and brightness of the star-field is well known in star catalogs, accurate knowledge of the satellite position and brightness can be deduced from this comparison. AstroGraph, developed by Paul Sydney at Boeing, becomes the key software tool for conducting the astrometry of data taken from the LEO Raven. Once accurate satellite observations have been conducted, this software will match the plate to the star catalog which finds the satellites' position. The software also conducts cosmic ray detection and subtraction.

Figure 30 shows the Astrograph screen after the stars have been matched to the existing catalog.

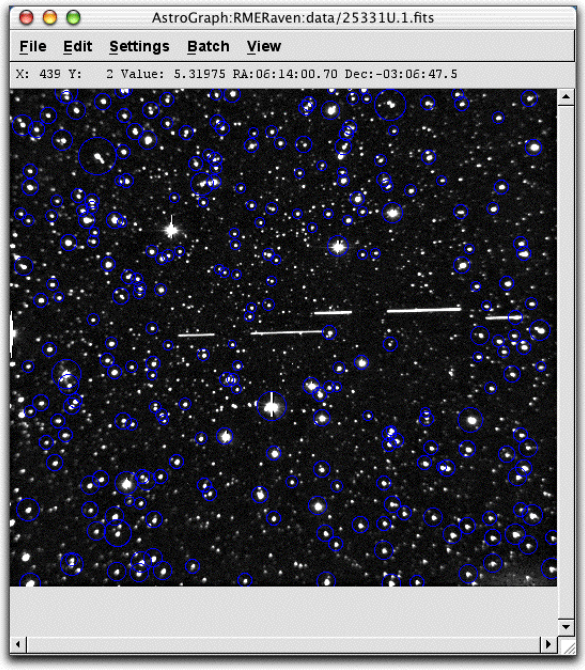

Figure 30. Astrograph

The process menus include: Image Display; Background Subtraction; Sensor Specification; Star Detection; Star Catalog (USNO/Tycho); Star Match (Plate solution); Object Map which uses the satellite catalog and flies from know objects; Object Detection (points or streaks); Object Correlation (to catalog); User Marking (manual); and finally, Reporting a AST File (Astrometry file with photometry). Each of these fields can be customized for the astrometric output. Visually this can be represented in Figure 31.

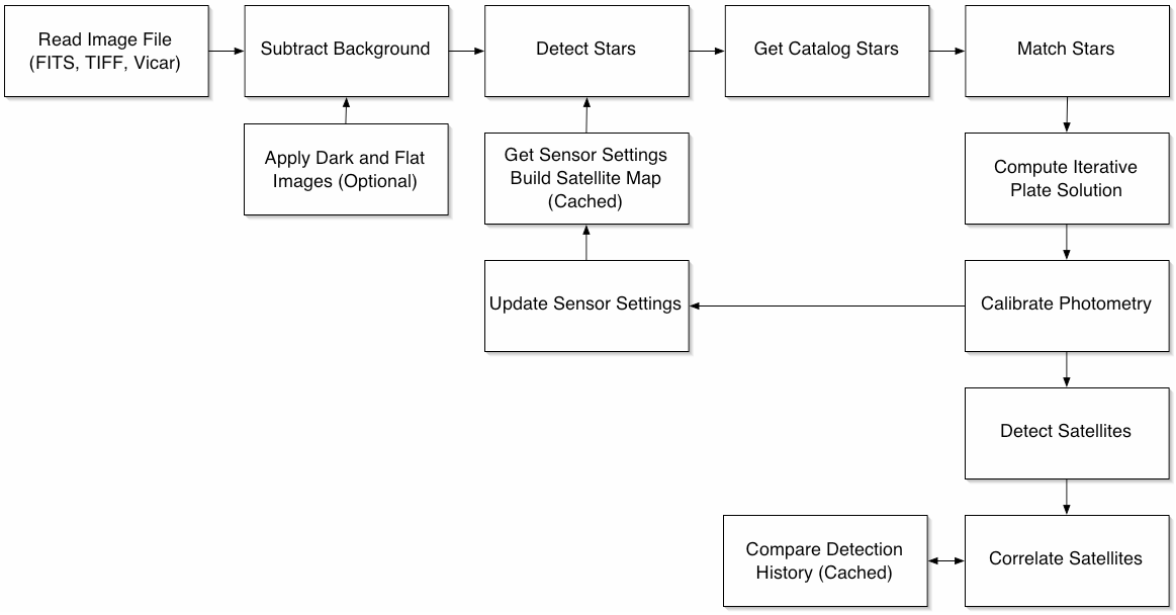

Figure 31. Astrograph Process

Note that the Star Match function utilizes gaussian triangle pattern matching (ratios and angles), pixels from world coordinate system (WCS) to Equatorial, and includes transformation matrix with a bias. AstroGraph outputs its information into GTDS, the Goddard Trajectory Determination Software. This software accomplishes the final orbit predictions, references, and final plots.

3.4 Summary

This space to detector model, hardware, and software lead to the research conducted at MSSS. Chapter 4 will explain what was accomplished through this three-pronged approach to designing a deployable, daylight LEO Raven system. The systems—the 0.42m HANDS, 1.60m GEMINI, and the 0.36m RME Raven—and the software tools will lay the ground work

for the LEO Raven. Questions answered will include: How fast can typical Raven/HANDS mounts track LEO satellites? How many stars could potentially be seen above the sky background, and can accurate astrometry be done? Can the current Raven observe LEO satellites during daylight with the Merlin camera configuration? If feasible, how much better can observations get with a different detector?

IV. Research and Analysis

The data collection component of this research consisted of three sets of experiments at the Air Force Maui Optical and Supercomputing (AMOS) site and follow-on modeling analysis at both AMOS and the Air Force Institute of Technology (AFIT). The first experiments addressed the issue: Can the existing Raven mount track LEO satellites? The second experiments sought to answer the questions: How many stars could potentially be seen above the sky background, and can accurate astrometry be done? The third experiments repeated many aspects of the second except using Raven-class hardware near sea level and addressed how effective the current Raven setup performed.

Research began on arrival at the Maui Space Surveillance Site on 13 Oct 2003 and concluded on 11 Dec 2003. Dr. Chris Sabol served as the associate advisor during the research at MSSS. Figure 32 shows the MSSS atop Haleakala with the 3.6 meter telescope in the background.

Figure 32. MSSS Observatory at 10,000'

Several other contractors assisted in my education process as well. They include: Paul Sydney, Technical Fellow for Boeing; Dan O'Connell, Optical Engineer for Oceanit; Mike Murai, Computer Specialist for Oceanit; and David Witte, AFRL infrared research support. Each of these individuals support the existing High Accuracy Network Determination System (HANDS) initiative and eagerly await the recommendations of the daylight LEO Raven experiments which will ultimately feed the extended-HANDS initiative. As mentioned earlier, the daylight LEO Raven experiments were conducted on the 0.42 HANDS Raven telescope, 1.6m GEMINI telescope, and the 0.36m RME Raven telescope. Section 4.1 begins with the initial experimentation using the 0.42m HANDS Raven telescope.

4.1 0.42m HANDS Raven Experiments

The LEO rate tracking experiment utilized the 0.42m High Accuracy Network Determination System (HANDS) Raven telescope located at the Remote Maui Experiment (RME) site near sea-level in Kihei. The 0.42m HANDS Raven telescope is shown in Figure 33. The approach was to track satellites in GEO during terminator and gradually attempted observations of satellites with increasing mean motion. Objects selected were based on available satellites at the time during the terminator hours. See Appendix A for an abbreviated simulation of the orbit pass.

Figure 33. 0.42m HANDS Telescope

As the mean motion increased beyond 6-7 revolutions/day, problems arose. TheSky software tracking is based off initial rate input with no updates to the rates. Since most LEO orbits are not perfectly circular, they introduce varying accelerations as they move through the orbit. With no rate updates, the software introduces tracking error as the orbit track progresses. There is also several seconds of delay between when the telescope track command is generated and the CCD camera begins to record an image. The results are that fast moving satellites begin to appear away from the center of the image and no longer appear as a point but are streaking due to the changing rate of the space object. The former problem could result in acquisition issues while the later greatly reduces astrometric accuracy. See Figure 34 for a 1 second exposure of satellite #22781 taken on Oct. 22, 2003 @ 0601 UTC.

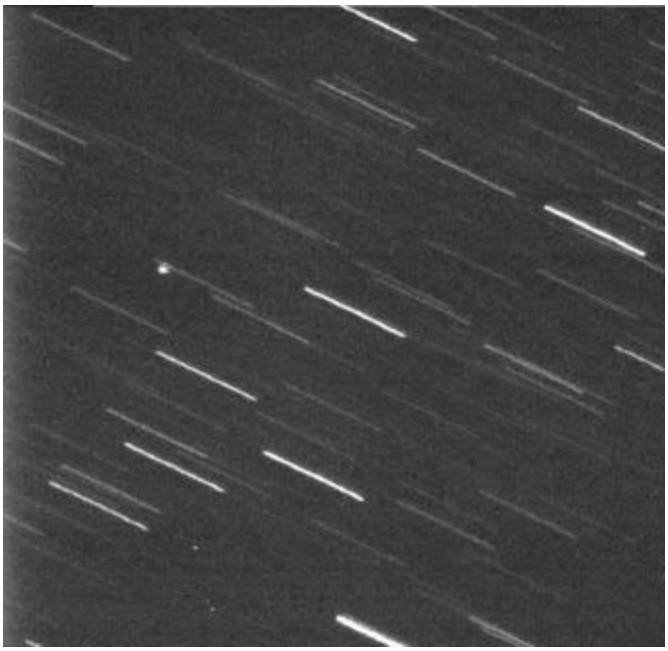

Figure 34. Sat #22781 taken on Oct. 22, 2003

The HANDS Raven did acquire a satellite (object # 22781) with a mean motion of 10.73 revolutions/day; however, it was moving relatively slow when acquired since its eccentricity was 0.24, and it was near apogee. Initial acquisition occurred at 0552 UTC, at which time it was traveling at -178.222 arcsec/sec in right ascension (RA) and -23.235 arcsec/sec in declination (Dec). The last acquisition was at 0604 UTC with a rate of -228.979 arcsec/sec in RA and -136.733 arcsec/sec in Dec. Clouds subsequently moved into the FOV, and the system was unable to reacquire 22781 starting at 0609 UTC. As a result of the problems mentioned earlier, the HANDS Raven telescope could realistically only track objects of 6-7 mean motion.

The limiting factor in this experiment was the implementation of the rate track option in TheSky. However, significant mount jitter also appeared in the images. For LEO Raven,

improvements to the rate track mechanism should be considered, as well as, modifications to the mount. The tracking and mount issues will be addressed in section 5.1. After the initial experiments on the HANDS Raven, astrometric attempts were made on the 1.6m GEMINI telescope using the Daylight Acquisition System (DAS).

4.2 1.6m GEMINI DAS Experiments

The primary sensor used for data collection on the 1.6m GEMINI is the Daylight Acquisition System (Digital output) or Indigo Merlin camera. Operations at the MSSS site used trained operators to run each telescope. Due to this setup, a scheduling request outlined the desired DAS observations, and while the observations commenced, I collected the data. Initial observations requested a sidereal track with star-fields taken at the start, culmination, and end of the pass. These star-fields need to be 5 seconds in duration with a record of right ascension and declination, mount angles for the entire pass, and metric marks. These star fields would provide background information for various places in the satellite pass. This information coupled with data throughout the pass will feed into the astrometry and orbit determination. In addition, the preferred objects include the laser ranged satellites mentioned in section 3.1.2.

Typical preparation for satellite observations included watching the weather and generating satellite pass lists. Plan Pass became the main source of this satellite pass information. Up on top at the AMOS observatory, operators took the scheduling request and satellite pass list to run the actually telescope hardware. As the experimenter, I sat in the control

room to monitor the operators and actually collect the data at the proper time. Appendix B contains a typical orbital element set and satellite pass list used for the 1.6m GEMINI experiments. Section 4.2.1 discusses the 1.6m limitations. Once the two line orbital element sets were acquired from AFSPC and the pass list was generated for that particular day, actual experimentation could begin! The experiments are listed via date of collection in section 4.2.2.

4.2.1 1.6m System Limitations

Prior to conducting experiments, it became apparent that the limitations of the sensor and 1.6m telescope system needed to be understood. The Daylight Acquisition System limitations included data acquisition limited to 90 seconds, data readout requires 2 minutes for that amount of data, overlapping passes will require a 45 second split, and DAS runs at 60 frames/seconds. In addition, the DAS on the 1.6m runs the old software and the output file is a stacked Flexible Image Transport System (FITS) file with no heading (which astrograph needs to do the astrometry).

The DAS sits on the 1.6m to act as an acquisition sensor for the main 1.6m GEMINI telescope, so these observations kept the current configuration. A more flexible configuration would have allowed a better Non-uniformity Correction (NUC) calibration and time tagging for the data. This would have provided more accurate photometry and astrometery. Since the largest source of error in the astrometry stems from the lack of time-tagging of images, a solution needed to be found to rectify the situations. The solution for this problem will be to have operators step the mount. In order to accomplish a timing mark, the mount will be

stepped off 5 arcseconds, the mount log reset (this records a time in the log), and moved back to the satellite. Once the data is processed, the observed step can be correlated to the recorded time in the mount log. This will allow a plate solution to be formed for the DAS detector and the timing will aid in producing the predicted orbit through astrometry.

4.2.2 Observations

10/27/03

First attempts at data collection occurred on October 27, 2003 at the MSSS observatory. Utilizing the 1.6m telescope, the DAS attempted to collect against several passes. Unfortunately, observations were weathered out by high cirrus clouds. Throughout our time window of 0100-0400 zulu, operators attempted observing catalog objects 22195, 22824, 7440, and 26977. Despite not acquiring the desired targets, several observations successfully imaged a few stars. Magnitudes consisted of zero, third, and fourth orders. While this helped with checking the accuracy of the pointing, no usefully astrometric data was collected.

As the weather continued to hamper observations, we explored calibration parameters of the DAS. Specifically, activities focused on how the automatic gain correction (AGC) affects data conversion from analog to digital signals. Exploration showed that the AGC is applied initially, but not updated. As a result, the system looses some of the correction initially applied, and with a changing sky background, this could limit the amount of stars and satellites seen above the background noise.

10/28/03

The following day, Oct 28th, second attempts at data collection occurred. Again, weather did not cooperate. Humidity levels required the telescope doom to remain closed. At high humidity levels moisture can condense on the optics which consequently peals the optical coatings. In addition, high cirrus clouds covered the site.

Despite "red" operations, operators helped collect flat-fields, dark-fields, and saturation data on the DAS. These experiments aided in the understanding of the DAS's non-uniformity correction (NUC) function. This NUC is an offset which subtracts a bias from the sensors images. Due to imperfections and peeling paint on the inner dome, moving the camera allowed for a more even flat-field. Next, a closed shutter allowed dark-field collections. This dark-field reveals imperfections and background noise inherent to the DAS charge-coupled device. Then, a saturation test showed the DAS limits. Using an interior dome light and looking at the inner dome, the DAS took an image which saturated as expected. Finally, we explored the DAS integration time settings, but due to the 1.6m GEMINI configuration these were kept as set by the telescope operators. Experiments on the 0.36m RME Raven provided a better opportunity to explore the integration time functionality of the DAS.

10/29/03

Activities on this day included submitting a scheduling request for the week of 3-7 Nov and attending the subsequent scheduling meeting. After the scheduling meeting, a few adjustments were needed in observation plan. MSSS serves several high-level customers to include AF Space Command and the Missile Defense Agency, which take precedence over my current experiments. As a result of AFPSC collects being behind for the month, the only day available for operations the week of Nov 3-7 would be Nov 7th, and observations would also need to be planned around AFSPC objects. Once the passes for Nov 7th were run, they showed no conflict with the AFSPC observations.

11/7/03 and 11/21/03

Successful data collection with the DAS-1.6m setup occurred on both days. The observation logs can be seen in Appendix C. Note that fog forced the closure of all telescope domes during the morning hours for the 11/21/03 DAS operations. As a result, the best SLR passes were missed. Later that afternoon, once the fog cleared, several collects were done on any available LEO satellites. The MSSS operators have their own software that shows all current objects over the horizon, and the can be easily selected for observation. This day of collection ended up being the final day of observation at the summit of Hakeakala on the 1.6m telescope.

These observations showed that the limiting magnitude of the 1.6m GEMINI-DAS setup fell around 8-9th magnitude. The data for 11/7/03 included star observations and satellites, but no stars streaked through the frames during collection. The data for 11/21/03 included 14 satellite collects with 7 of them having stars streak through the FOV while collecting data. While more satellite/star combinations would have been desired, this provided an initial good look into astrometric design characteristics for the LEO Raven. These design implications will be discussed in section 4.4.

4.3 0.36m RME Raven Experiments

While conducting experiments on the 1.6m DAS system, it was discovered that a spare DAS Indigo Merlin camera was on site. The MSSS engineering team allowed this research effort to borrow the camera for 10 days for use with the RME Raven. The RME Raven telescope seen in Figure 35, which is different from the HANDS Raven also located at RME, is a 0.3625m, f/3 Torus Optics Newtonian telescope with an open framed truss on a Paramount MME German-Equatorial mount. A custom made adapter had to be manufactured to mount the DAS on the RME Raven and was completed by the Maui Optical Sciences and Imaging Application Center (MOSAIC). Specific system parameters of the RME Raven and Merlin setup can be seen Table 11. Note that the FOV at 0.498 x 0.398 degrees is similar to the DAS on the 1.6m at 0.5 degrees.

Figure 35. 0.36m RME Raven Telescope

Table 11. RME Raven FOV with the Merlin Camera

Focal Length	1.1049022		meters (m)
Detector Size	320	256	Pixels
Pixels	3.00E-05	3.00E-05	m
Length	9.60E-03	7.68E-03	m
FOV	4.98E-01	3.98E-01	degrees
	2.99E+01	2.39E+01	arcmin
	1.79E+03	1.43E+03	arcsec
IFOV	1.56E-03	1.56E-03	degree/pix
	5.60E+00	5.60E+00	arcsec/pixel

The initial test plan included looking at established Langholt star-fields (known calibration fields) to see the magnitude limits of the DAS camera on the RME Raven (8-9

magnitude on the 1.6m). This could be done by observing from 1600-2100 local taking star-fields throughout the entire pass which would help characterize the system in daylight and into terminator conditions. The goal was to see some satellites during daylight, observe stars, and some possible terminator data. At the time, no Langholt star-fields were on hand, so observations were made of other known stars. Figure 36 shows an image of the moon taken with the Indigo Merlin-RME Raven setup.

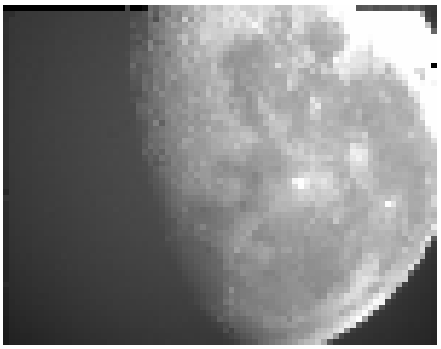

Figure 36. Moon Image from the Merlin/RME Raven setup

As mentioned above several challenges existed with mounting the DAS camera on the RME Raven. Dan O'Connell from MOSAIC supplied an existing C-mount converter, shown in Figure 37, to mount the camera. Once the Merlin camera was mounted on the Raven, the system had to be re-balanced and focused. Other modifications will be discussed under the activities of November 12th.

Figure 37. C-Mount Adapter for the Merlin Camera

11/5/03

Initial observations during the late afternoon and evening on 11/5/03 indicated the RME Raven-Merlin Camera setup had very bad vignetting which limited the usable field. The warm metal dome reflected large amounts of radiation, and with no shrouding on the telescope, stray light severely limited the Merlin's detection threshold. The camera also saturated immediately when clouds passed through the FOV. Thankfully, the software allowed for using a region of interest with the camera which reduced the background and got the image away from the vignetting edges. In addition, observations revealed substantial jitter at 1 pixel or ~5.6 arcseconds! Atmospheric distortions can account for some of this, but mount instability accounts for most of this jitter. Future LEO Raven designs must ensure a more stable mount to reduce the error of the orbit predictions.

Initial observations at 4:10pm, observed a 4.67th magnitude star, #103285 and spectral type K0II-III, with a 4.5ms exposure. At 1730 closer to sunset, a 7th magnitude star became easily observable, but the desired 8-9th magnitude stars were not observed during daylight

hours. On a new system with no vignetting (optical distortions at the edges of the optics), better baffling (pieces that block straying light from entering the detector), frame co-adding (post processing which increases the final signal output), and background subtraction (taking out the relatively constant background noise) observations of 8-9th magnitude stars should be possible. Figure 38 illustrates a typical star observation. Notice the limited dynamic range of the detector which reduces the signal strength above the background noise.

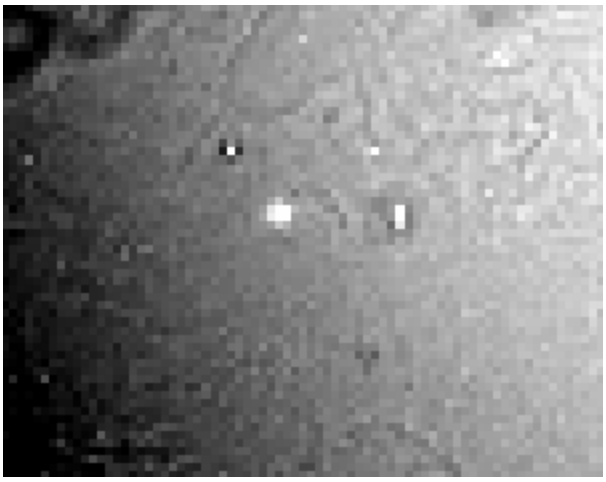

Figure 38. Eltanin collected on 14 Nov

11/12/03

The goal of these observations was to explore the Raven-Merlin combination, find limiting magnitudes of stars, and attempt to track some satellites. If everything worked perfectly, some astrometry could be done on the satellite-star observations. Satellite pass preparation revealed several morning passes for observation with the RME-Merlin setup. Figure 39 shows clouds filling the FOV and saturating the Merlin detector.

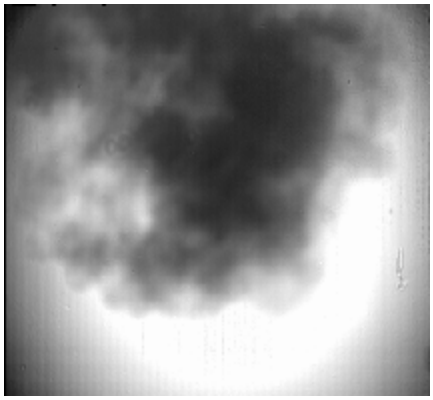

Figure 39. Clouds Saturating the Merlin Sensor

Observations showed that the limiting magnitude during the daylight hours was 6.33. Satellite passes were attempted, but they were met with no success.

After noticing the straylight and baffling problems due to the lack of a telescope shroud and sunlight reflecting around the dome, a few modifications were made to the telescope frame and dome. Dan O'Connell from MOSAIC supplies some black canvas material which we custom fit to shroud the Raven telescope, and some of the material was hung from the dome slit in order to block in coming sunlight from bouncing around in the dome. Figure 40 illustrates these modifications.

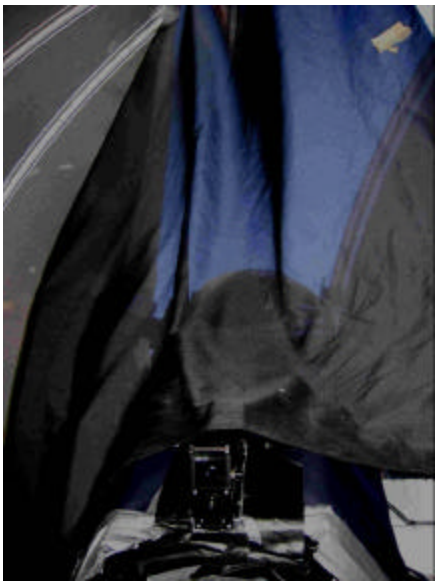

Figure 40. Telescope Shroud for RME Raven/DAS

11/14/03

Observations again attempted to acquire satellites and observe stars. Shrouding improved the systems' ability to image during daylight by one magnitude. Observations successfully acquired a 7.41 magnitude star. A possible satellite collect occurred while viewing Eltanin, star 30653. An object passed through the field of view (top left to bottom middle) and created a halo (like water spots). Further analysis revealed that this was a reflection from the dome or optics, not a satellite.

Later in the observation period, sky background brightness and clouds reduced the ability to observe dimmer objects. The Raven system could not see 6.01 or 5.72 magnitude stars. The slit coverings, while helping reduce the dome reflections, eventually fell off. In addition, even movement of the slit coverings in the breeze reflected enough light into the

telescope to be noticeable. Due to time constraints and wind, observations were better with the slit covering off, but a future LEO Raven will need to have a specially painted dome to reduce these reflections.

Observations on the 14th also attempted to sidereal track and let a satellite pass through the FOV. While collecting on satellite #23560, a point in TheSky was picked in front of the satellite. The goal was to hopefully get the satellite to pass through the FOV. This approach did not work due to the limited FOV of the Raven-Merlin setup and the inaccuracy of the two line element sets. These observations concluded the daylight collection with the RME Raven and Merlin camera configuration, but a few night observations were made to hopefully provide some information for creating the a plate solution for the astrometry. The plate solution basically maps the x,y pixel space of the detector to equatorial coordinates. The solution includes the arcseconds per pixel, nonlinear terms of the optics, and any other optical aberrations.

While setting up for these November 14th night observations a satellite streaked through the FOV, but unfortunately the image capture software was not recording. Although, satellites are easier to observe through terminator, these observations focused on collecting frames with two stars (not a binary) close together in order to see the plate scale. One Figure 40 shows satellite 26977, COSMOS 1191, moving slowly, but this was just a Molynia orbiting satellite that was available during the observations. Figure 41 also shows the two star plate solution collect, and see Appendix D for the specific list of collections for these observations.

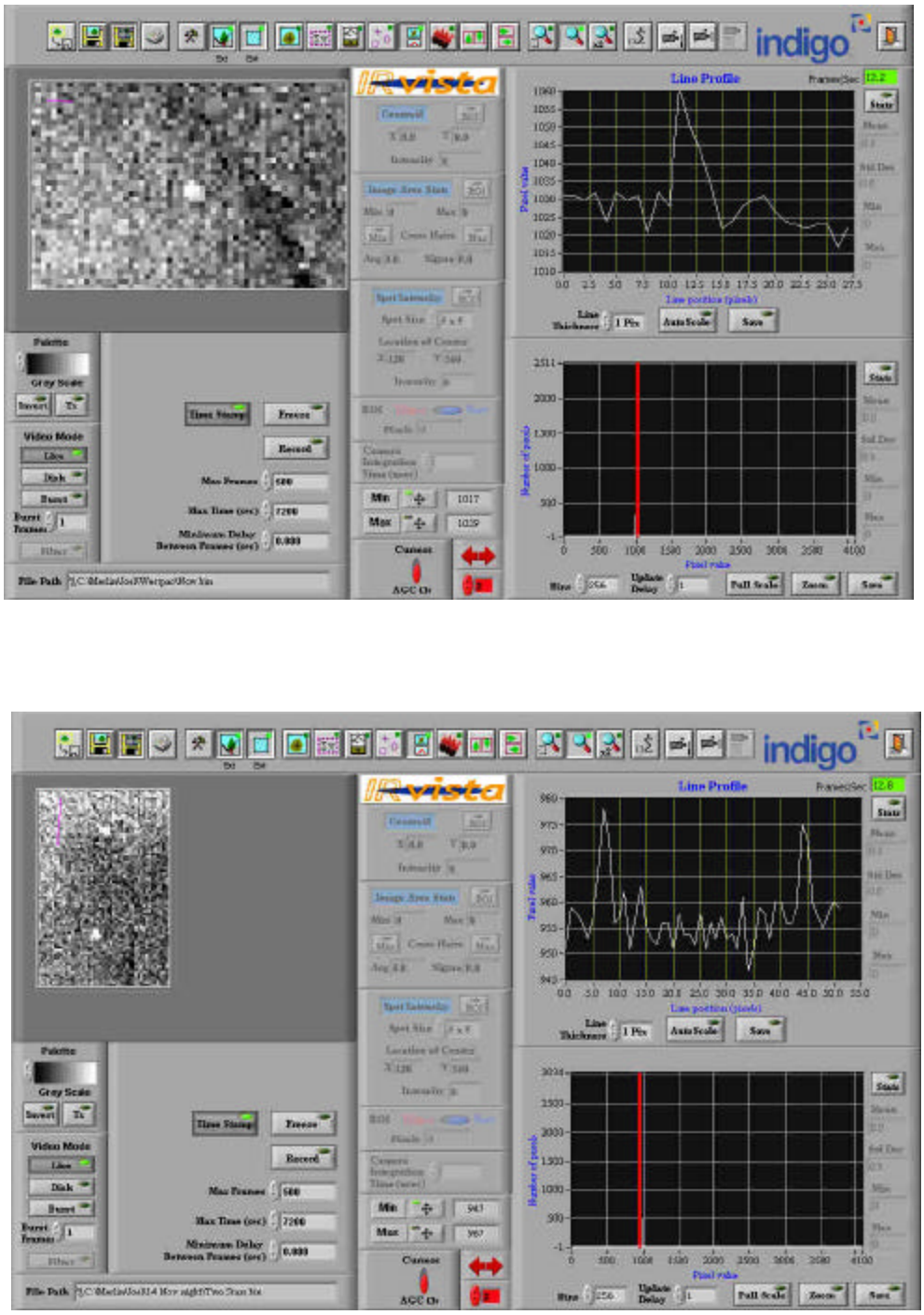

Figure 41. COSMOS 1191 satellite observation (#26977) (a) and Two Star Collect (b)

These night collections finished off the experiments on the RME Raven. The camera needed to be returned to the observatory up top for integration into the MDA test approaching on 11 Dec. The following sections, 4.4-4.7, explore analysis of the 1.6m GEMINI data and the 0.36m RME Raven data.

4.4 Astrometric Analysis

Data collected on the 1.6m GEMINI was hoped to provide some accurate astrometry results. Due to weather, software, and hardware configuration issues, good data was not obtained to accomplish this effort. Despite the marginal data, an attempt at the astrometry and orbit determination was made. One particular 1.6m DAS observation on 21 Nov obtained three stars passing through the FOV while collecting on satellite #15369.

Since the data was not tagged with accurate timing data, a manual examination of the data ensued. Frame by frame analysis revealed where the telescope stepped and the time tag in the log reset which occurred at 23:29:10 UTC. From that reference times for the star passages were calculated. One of the stars passed through the FOV when the log reset, so it made matching times to frames a little easier. The frame rate was set at 30 frames/second, so 30 frames would equate to one second. Through the observation of this pass, each star passed through the FOV approximately 1.5 seconds apart. Table 12 shows the analysis of these frames.

Table 12. 21 Nov, Sat 15369 Try #1

Star	Frames in View	Duration (seconds)	Frames Separation	Between Time
#1	189-233	1.4666667		
#2	284-300	0.5333333	51	1.7
#3	343-375	1.0666667	43	1.433333

The star pattern flowed across the screen in the order of top, bottom, top and with a brightness of medium, brightest, and dimmest. Next, a two line element set for satellite 15369 was loaded into TheSky and set for that date and time. TheSky provided a means to step through the pass and look for that particular star pattern.

Usually when conducting astrometric analysis, the analyst sees tens if not hundreds of stars in the collect for accurate star matching. In this case, there were three stars coming through the FOV at separate times. In addition, the accuracy of the two line element set might introduce enough error to never find the correct stars. The two line element set used to generate this pass were from 21 Nov 03, but due to the generation process and delay in accurate updates, the following star patterns may be mismatched. Needless to say, around the time of observation and imposing the 8-9 magnitude limit of the 1.6m DAS system. Table 13 shows the possible star combinations.

Table 13. Possible Star Combinations for the 15369 Pass

SAO	Mag	Type	Time
68766	7.32		23:29:04
48789	6.36	M	23:29:06
48845	8.38	F	23:29:08
48876	8.42	A	23:29:10
48891	7.15	K	23:29:12
48961	8.24	K	23:29:14
48961	8.24	K	23:29:14
48962	8.01	A	23:29:16
49042	8.41		23:29:18
68751	6.37	K	23:29:02
48737	6.22	A	
48789	6.36	M	

The first star pattern listed is the most likely match for this star pass. Usually, AstroGraph takes the data and automatically matches the stars to the known catalog. In turn it applies the correct transformation matrices to come up with the coordinates of the satellite. Since this data did not have accurate timing and was not a laser ranged satellite, even if the orbit were found, there would be no accurate reference orbit to compare it against.

While the goal of completing daylight astrometry experiments with the DAS was not actually realized, several important things were learned in the process. Primarily, while a few stars would pass through the DAS FOV during the course of a pass, it would be desirable to

have many more. This indicates that LEO Raven should attempt to incorporate a wider FOV, a more sensitive CCD, and maybe consider a 1m class optical system. Secondly, even with the above considerations, astrometry for the LEO Raven will likely be much more rudimentary than what is employed by the deep space Raven. With the deep space, visible sensors, the ten to hundreds of observed stars allow for the astrometric processing to directly estimate plate scale, orientation, and many other parameters for each image. For LEO Raven, many of these variables may have to be measured outside of the satellite track while only one to a small number star are available to calculate offsets from the nominal trajectory. Clearly, more astrometry experiments will be required in the future.[29]

The analysis that follows in section 4.7 will focus on radiometric results of the RME Raven versus the astrometry efforts on the 1.6m GEMINI. The analysis stars with exploration of different atmospheric parameters encountered and a discussion on the detector itself. Ultimately, the RME Raven experiments fulfilled the research goals and provided a better understanding of a new LEO Raven design. Despite the lack of astrometric data, the 1.6m experiments helped in understanding DAS (Merlin) camera performance parameters and overcoming collection software issues which aided in a more productive time with the RME Raven.

4.5 Detector Performance Analysis

The following performance analysis of the DAS on the 1.6m GEMINI highlights the challenges of the current Merlin camera. Doyle Hall from the Boeing Company conducted

these calibration tests in early 2003. Below are some of his concerns relating to the radiometric capabilities of the DAS camera, many of which affected the LEO Raven research and development.

> Unfortunately, the current DAS system probably needs to be re-calibrated during/after every use. In other words, the zero-points vary from night to night. This is not true for most astronomical detectors, which experience relatively slow zero-point changes as devices age and lose sensitivity. The need for the DAS re-calibration is probably due to the NUC (non-uniformity correction) procedure used in the DAS camera. The NUC procedure attempts to account for non-uniformities of the signal on the detector, mostly in order to make a more cosmetic image. Unfortunately, the NUC procedure seems to have the unwanted effect of re-initializing the detector zero-points. So DAS NUC procedures should never be performed *during* an observation shift, so that all calibration stars are acquired using the same NUC parameters as the target objects.

Future analysis of the Merlin or a similar camera needs to address how the signal rates for constant sources (like bright stars, for instance) vary considerably as a function of position on the detector. These effects are related to the NUC and must be thoroughly understood before implementing a detector like this in the LEO Raven. In addition, constant recalibration of a LEO Raven would limit its ability to operate autonomously.

At the present time, the Indigo Merlin (DAS) camera would not be adequate enough for use on the LEO Raven due to its limited dynamic range and non-uniformity correction. Indigo has developed the next generation NIR detector called the Indigo Phoenix. MSSS purchased one of these detectors and plans to characterize it for use in the active track program. Data collection did occur with this detector on the 3.6m AEOS system, but operators inadvertently

recorded data on a classified object. As a result, the data could not be used in this thesis for a comparison of the Merlin and Phoenix cameras.

Looking at Indigo's published specifications, the Phoenix has a better well-depth (deeper) while the Merlin's well-depth fills up faster with background noise. Consequently, the Phoenix boasts a better dynamic range which would allow longer integration times and a better signal to noise ration. Initial estimates based on limited Phoenix data collection places its performance at 2x that of the Merlin detector. Further experimentation for the LEO Raven should utilize the Phoenix detector and better understand the non-uniformity correction function of the camera. To ensure accurate astrometry results on the LEO Raven, the final systems should use the Indigo Phoenix camera and consider investing more money in a better detector. Despite the final LEO Raven configuration, the system must deal with atmospheric effects. Section 4.6 analyzes the atmospheric effects encountered in the LEO Raven research and highlights the worst case scenario for atmospherics at the RME Raven site.

4.6 Atmospheric Analysis

As a deployable system, the LEO Raven must be able to operate in many different climates. Operating in different areas introduces varying atmospheric transmission of the reflected satellite and stellar radiation and also multiple background variables. These sky background variables include geography, season, topographic features, time of day, scattering angle, altitude, weather, and spectral band. The current location of the RME Raven provides one of the most challenging microclimates for the Raven to operate. Its location at sea level and

proximity to the ocean introduce the maximum atmospheric effects and reflection from the ocean. This maritime climate contrasts greatly with the 1.6m GEMINI telescope at MSSS which is located in a desert microclimate and above much more atmosphere at an altitude of 10,000 feet. Overall, these two locations provided a good comparison of different operating climates.

The following graphs are a MODTRAN simulation, an atmospheric modeling tool developed by the government, of how much radiation passes through the atmosphere for a maritime environment on Maui for the RME Raven site (the lower curve in green) and a desert environment for the 1.6m GEMINI system at the summit of Haleakala (the higher curve in red). Parameters for the RME Raven sit include: latitude, 20 deg 44m 46.32s, and longitude, 203 deg 34m 05.88s east. The altitude is at sea level, a zenith angle of 40 deg, azimuth of 30 deg, and end path of 80 km. Finally, the time set to 19:30 UT daylight or 0930 local. The 1.6m GEMINI simulation graphs the atmospheric transmission and radiance for the GFO pass on 7 Nov 03 at 2100 UT or 1000 local. The latitude was set at 20 deg 42m 30.138s and the longitude at 203 deg 44m 33.517s east. The altitude sits at 3060.54 meters, with a zenith angle of 40 deg, azimuth of 30 deg, and end path for 80 km. Figure 42 shows the atmospheric transmission comparison of the 1.6m GEMINI and 0.36m RME Raven. The red trend-line represents the 1.6m GEMINI, and the green trend-line reflects the RME Raven.

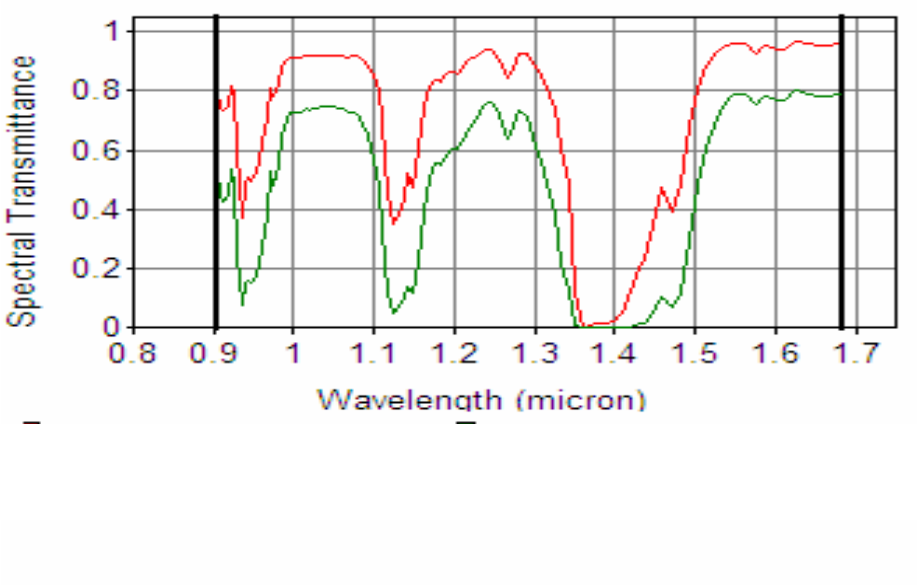

Figure 42. Spectral Transmittance for MSSS (Red) and RME (Green)[28]

From the comparison see that the atmospheric transmission accounts for another 20% reduction in signal for a system at sea level versus 10,000 feet. Figure 43 compares the spectral radiance of the sky for each location. The RME Raven is in green and the 1.6m GEMINI location is represented in red.

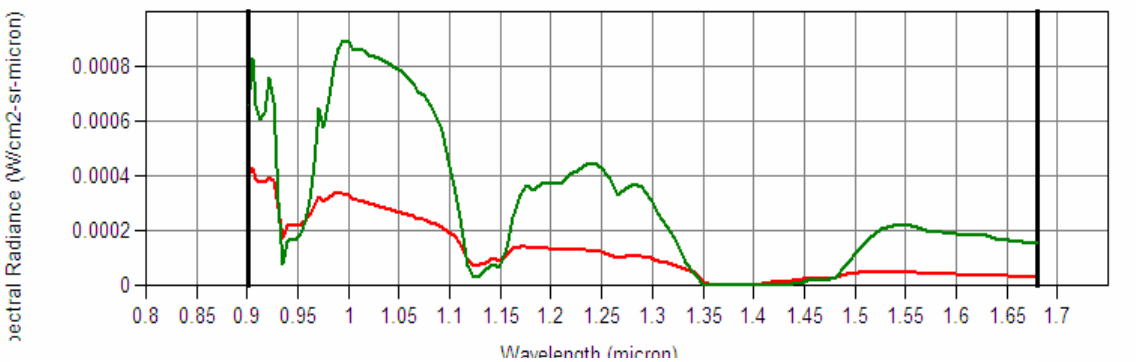

Figure 43. Spectral Radiance for MSSS (Red) and RME (Green) [28]

The effects of increased water vapor and reflected ground radiance at sea level cause a higher spectral radiance for the RME Raven. Reflected ground radiance is especially dominant in the near infrared which will introduce more noise for a detector, especially in a maritime environment.[13] If at all possible a deployed LEO Raven should sea level locations and look for a higher altitude observation point.

Since the LEO Raven will be a deployable system operating in many microclimates, a few other simulations were run on data comparing a desert and maritime climate at the RME Raven location. Although, the maritime scenario will always be the limiting factor due to the increase in available water vapor (at sea level) and solar reflectance off of the water's surface. Figure 44 shows this desert and maritime comparison.

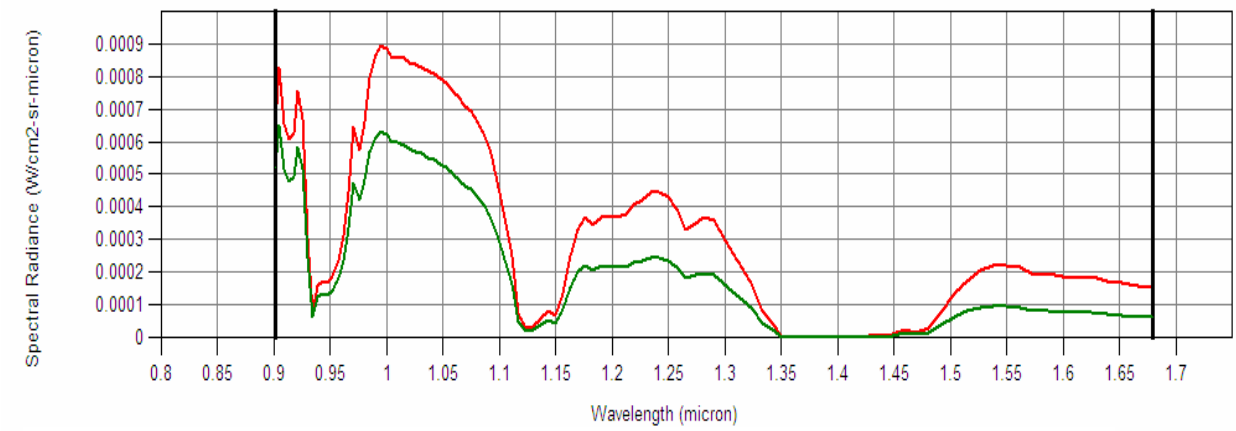

Figure 44. Spectral Radiance at RME for Maritime (Red) and Desert (Green) [28]

Notice that the spectral radiance is about 20% greater in a maritime environment. The RME Raven operates in this harsher environment, so it provided a good backdrop for the worst case scenario for a LEO Raven system. The following radiometric analysis in section 4.8 looks at a daylight case with an elevation angle of 20 degrees which also introduces more atmospheric losses for the incident radiation.

4.7 Radiometric Analysis

In an effort to correctly scale these observations to a potential LEO Raven, a radiometric model was developed to accurately reflect the observations with the 0.36m RME Raven and Merlin Camera. The star chosen for analysis was SAO 103285, Spectral Type K0II-III, with a magnitude of 4.67 and was observed on 11/5/03. The following process uses the end-to-end approach outlined in section 2.7.

4.7.1 Predicted Data

Step #1: In order to get an estimate of the calculation, irradiance values for Vega were used to scale the irradiance to SAO 103285. Astronomers have thoroughly characterized the spectrum for both Vega and Sirius for use in radiometric comparison. Astronomers consider Vega a 0^{th} magnitude star for all intents and purposes (actual visual magnitude ~0.03). Values from the Cohen irradiance database were used to fit an equation and calculate the total

irradiance from the Merlin spectral band pass of 0.9 to1.68 microns. The total estimated exo-atmospheric irradiance for the 0.9-1.68 band pass was calculated to be $2.67*10^{-13}$ W/cm^2. Figure 45 represents the Cohen database values and subsequent blackbody approximation.

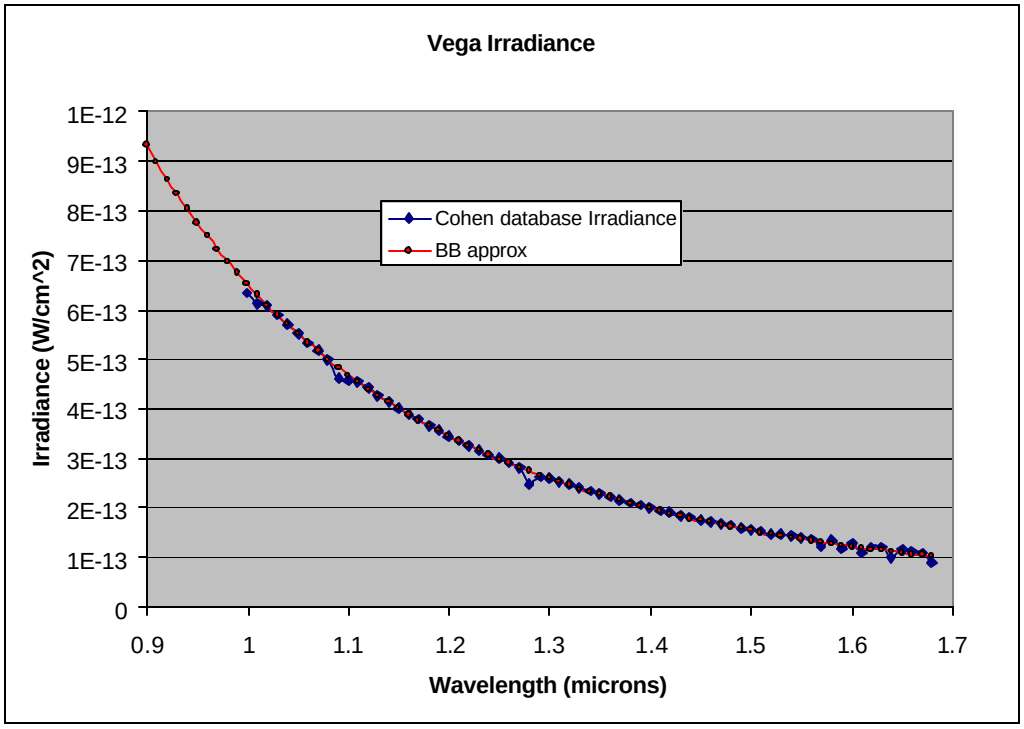

Figure 45. Vega Irradiance

Step #2: Once the exo-atmospheric radiance of Vega was found, it needed to be scaled to the observed 4.67 magnitude star. The following equation represents the transformation to the equivalent irradiance using the irradiance values of Vega (I_λ), magnitude (m_o) of the observed star, and magnitude of Vega (m).

$$m = m_o - 2.5\log(I / I_o) \qquad (4)$$

$$I_o = I_l / 10^{(m_o - m)/2.5} \tag{9}$$

Step #3: The irradiance (E_λ) at the observation site can be found by multiplying the exo-atmospheric irradiance (I_λ) by the atmospheric transmission (t). The case turns out to be one of the best to use for this analysis due to its low elevations angle of 20 degrees.

$$E_l = I_l t_{atm} \tag{10}$$

Step #4: Incident power on the detector (ϕ) must account for the obscuration by the secondary mirror (A_s) and the transmittance of the optics (t_{optics}).

$$f = E_l A_p (1 - A_s) t_{optics} \tag{11}$$

Step #5: Next, calculate the number of photons being received per unit time. This can be found by taking the power received (ϕ) divided by the energy per photon. See Table 7 for these values.

Step #6: Multiply the number of photons per unit time by the efficiency at which the device converts photons to electrons, which is the quantum efficiency (electrons per photon). And lastly, multiply the product by the gain of the detector to determine the signal ready for display

Step #7-10: These steps account for the integration time of the detector and the analog to digital conversion process. The volts per electron values were published by Indigo, but after several unsuccessful attempts at learning about the detectors A/D conversion process, an estimate for the detector voltage range had to be estimated. The counts are known since the detector is 12-bits or 4096 counts. Table 14 summarizes the calculations used for the RME Raven Merlin observations of star SAO 103285.

Table 14. RME Radiometric Analysis

f/#	3			
Optical Transmission	0.8281		Radius	
Diameter Primary (inches and meters)	14.5	0.368300737	0.18415037	meters
Diameter 2nd	5	0.127000254	0.06350013	meters
Focal Length (inches and meters)	43.5	1.10490221		
Step#1				
Find exoatmospheric radiance of Vega in the 0.9-1.68 Band Pass			**2.67E-09**	**W/m^2**
Step#2				
Scale to the observed star mag 4.67	4.67	Magnitude	**3.72E-11**	**W/m^2**
Step #3				
Find Irradiance on the ground			**1.86E-11**	**Scaled Value**
Transmission (via Plexus)	0.5			
Note: Star at 20 degrees elevation				
Step #4				
Find the Power at detector			**1.9606E-12**	**Watts**

Radius of the primary	0.1841504	m		
Radius of the secondary	0.0635001	m		
Optical Transmission	0.8281	m		
Step #5				
Find the # photons per time (=Power received/Energy per photon)			**1.22E+07**	**Photons/s**
Power received	1.961E-12	J/s		
Energy per photon	1.60E-19	Joules		
Step #6				
Find Electrons/time (= Q.E.*Gain*#photons/time)			**8.57E+06**	**Electrons/s**
Quantum Efficiency	0.7	electrons/photon		
Gain	1	unitless		
Step #7				
Take the integration time and multiply step #6 by that value	3.60E-03	seconds	**3.08E+04**	**Electrons**
Step #8				
Responsivity for the Gain Setting (A/D conversion factor)	1.70E-07	volts/electron	**5.24E-03**	**Volts**
Step #9				
Merlin is a 12-bit detector	4096	counts	**20480**	**Counts/volt**
Include the voltage range of the detector (estimate)	0.2	volts		
Step #10				
Find the final Counts!			**1.07E+02**	**Counts**

With a complete model, the actual observed data was analyzed and compared to the predicted values. Section 4.7.1 discusses the observed data.

4.7.2 Actual Observed Data

In the actual data, the observed star spread out over 4 pixels on the detector. Raw pixel data from this observation can be seen in Table 15. The data came from frame 61 of this particular collect and was displayed in the IR Vista software.

Table 15. Counts on the Merlin

Value	Background	Net
3435	3395	40
3430	3395	35
3470	3395	75
3445	3395	50
	Total Value:	200

The observed value of 200 counts reveals that the predicted value from Table 7 of 107 counts falls within an order of magnitude.

Several other observations were tested with the above method. Table 16 below shows the first test case compared to three other observations. The first two were taken during the daylight, while Vega and the dual star were collected at night. Observation of a K or M-class star may introduce more energy since its peak emission (compared to Vega an A-class star) falls closer to the Merlin detectors' band pass. The model design utilized a conservative approach, so the predicted values all fell under the observed counts.

Table 16. Comparison Star Observations

Observation	Predicted Counts	Observed Counts
Test Case	107	200
Eltanin	55.4	2006
Vega	4800	12000
Dual Star	68.9	296

This subsequent comparison helped validate the model and allowed for further exploration of the LEO Raven design space.

Changing the model in Table 7 to one with a 1m aperture, f/3, and secondary of 0.3m, the output counts will jump almost one magnitude greater (7 times better) while a 0.5m system will not produce much more performance than the current 0.36m system. As observed in the astrometric attempts, producing a LEO Raven with a wider FOV will be important, so the LEO Raven design should use a 1m telescope.

4.7.3 Error Analysis

Several of the parameters in Table 14 are estimates and may vary over a given location or time of day. Changing variable parameters in Table 14 for the atmospheric transmission and voltage range of the detector will change the outputted predicted value, but typical values remain within an order of magnitude. This shows that the model will be a good model to use for scaling

parameters to a LEO Raven design. In addition to varying parameters, many sources of error and background noise for the observations and analysis exist. They include:

- Sky Background/Radiance
- Atmospheric Turbulence and Transmission
- Detector Integration Time and Responsivity
- Unknown Processes in the A/D Conversion of the Signal
- Reflections off the water and dome
- Heating of the dome and the Merlin camera
- Spectral Class of the Observed Star
- Earthshine adds approximately 10%+ to the reflected radiation.

The current model in Table 14 accounts for many of these potential errors and the final design recommendations address ways to reduce these errors. Added together many of these background sources of radiation will affect the signal to noise ratio of the system.

As far as noise in the background, shot noise dominates. Shot noise is due to the random arrival rate of background photons. Higher integration times will reduce this source of noise but not all together eliminate it. Since the electrons reaching the detector mostly come from the background and other photon sources are small, the background limit of the detector can be estimated by the square root of the total background electron count. For the case mentioned in Table 15, the background noise can be estimated as the shot noise and is the square root of 3395 or 58.27 while the signal is 200. This leads to the signal to noise ratio

(S/N) which is an indicator of the statistical significance or uncertainty in the measurement. (110:221) The resulting signal to noise ratio for the observed case is 3.43.

Overall, a LEO Raven system design must accomplish an S/N ratio of 3 for the accuracy of its collection capability. Accomplishing only an S/N of 3.43 on a 4.67 magnitude star during daylight observations with the current Raven system is not sufficient. A LEO Raven system will need significant improvements to acquire and image a LEO satellite ranging from 6-9 orders of magnitude. These design considerations have been mentioned throughout this document and will be discussed in summary throughout Chapter 5.

4.8 Conclusion

Overall, the daylight LEO Raven experiments using the 0.42 HANDS Raven telescope, 1.6m GEMINI telescope, and the 0.36m RME Raven telescope provided powerful insight into the future design of a system. Despite the lack of actual astrometry, the astrometric analysis, detector exploration, atmospheric analysis, and radiometric results contributed a better understanding of the LEO Raven design challenges. Chapter 5 summarizes the LEO Raven design considerations and answers the questions posed in Table 1, addresses cost figures, explores future research, and wraps up this LEO Raven design study.

V. Discussion

This thesis presented the LEO Raven design approach that examined commercially available hardware components to determine if a low-cost, autonomous, astrometric sensor can effectively track LEO satellite in daylight conditions. Three data collection experiments and modeling and simulation analysis answered the four fundamental questions tied to the design trade space. Table 17 outlines the answers to these questions posed in Table 1.

Table 17. Answers to the Questions Posed in Table 1.

1	Objects move much faster in LEO which presents field-of-view and imaging duration challenges, so can the system track fast enough for LEO objects?
Answer	Current commercial mounts can track fast enough but are limited due to software and mount stability. For LEO Raven, improvements to the orbit prediction software must be considered. Additionally, efforts will be required to improve the telescope mount stability, so it will be better suited to LEO tracking.
2	Observations will need to occur in the 1-1.5 micron range (NIR), effectively "filtering" out the blue sky. Question: Can an adequate number of stars be seen, above the sky background, in a singe field-of-view in order to accomplish the astrometry?
Answer	Current FOV configurations limit stars for an astrometric analysis, but with an accurate mount model, the astrometry could be done with only a few stars. The LEO Raven must utilize a wider FOV (1m vs a 0.5m system) to increase the number of available stars for astrometry. In addition, the improving the timing and pointing accuracy of the mount will ensure accurate astrometry even with fewer stars.
3	What characteristics will be essential in a NIR camera and telescope system to be used for daylight observations? Is the current Merlin camera and Raven telescope configuration adequate? What improvements are possible with a different detector?
Answer	While other detector materials and spectral band passes are available, the InGaAs detector is a good commercial choice. The future NIR camera must be better than the current Indigo Merlin. The Phoenix

	will introduce about a 2x improvement in sensitivity/dynamic range. Having a greater dynamic range, the Phoenix will allow a longer integration time which increases the signal over the noise. Future experiments should utilize this camera, but even a more capable camera should be considered for the final design. Additional camera functions (i.e. the non-uniformity correction and automatic gain control) should be limited for a simpler, autonomous system. In addition, much of the radiation above 1.33 microns never reaches the detector due to lack of atmospheric transmission. As a result, the future LEO Raven should consider filtering out the 1.33-1.68 micron region.
4	Finally, given the answers to these questions, can an accurate system model be created in order to scale the results to the parameters of a future deployable LEO Raven?
Answer	Yes, the model shows that a 1m telescope will increase the sensitivity of the system by one order of magnitude. In addition, a more sensitive detector, like the Phoenix, will increase the number of observable stars and satellites by 1-2 orders of magnitude for astrometry.

In addition to those answers, the experiments uncovered unanticipated challenges for the LEO Raven such as:

- The length of data collection and download time for the data will need to be addressed, especially acquiring data on faster moving satellites (you need a long pass to fit the orbit on an unknown orbit, especially the eccentricity)
- Bad vignetting occurred on RME Raven which limited the usable field
- Telescope needs to be shrouded and baffled to increase performance
- The current metal domes heat up and reflect too much radiation, so a future system will need paint or a different covering, if it uses one at all.

- Smaller pixels and/or better matched to the optics is desired since current images are “swimming” in a pool of noise at 5.6x5.6 arcseconds

Discovering these issues led to the final design considerations outlined in section 5.1.

5.1 Design Considerations

Further development must address the optical design of the LEO Raven telescope system to include: telescope aperture, focal length, throughput, obscuration, vignetting, coatings, scattering, aberrations, ghosts, baffling, temperature swings, focusing, field of view, instantaneous field of view, spectral filters, and polarizers. Stemming from this research

- An aperture of 1m will increase the FOV
- Quality optics will transmit more radiation (increase the signal) and limit optical distortions (increasing the usable FOV)
- Coatings and/or filters can reduce the effective spectral band pass to 0.9-1.33 microns
- Baffling and shrouding the telescope will reduce the straylight and improve detection of stars and satellites
- A larger detector array (smaller pixels) will reduce the arcseconds per pixel and increase the accuracy of the astrometry.
- Future experiments could explore the added benefit of a polarizer to increase the satellites signal over the sky background.

Overall, much attention should be placed on the baffling and shrouding of the new telescope, finding a better detector, and increasing the FOV.

Detector considerations need to address the following desirable characteristics: responsivity (the higher the better), spectral response over the chosen spectral band, response time (time required for the detector output to change from 10% to 90% of its final value as a result of a step function input), linearity, quantum efficiency (higher the better), noise (lower is better), and detectivity. The Indigo Phoenix will be a better camera for future LEO Raven experiments, and even a newer detector should be considered. The newer sensor should use a non-uniformity correction device that is well understood, respond quickly to the incident photons, limit the spectral band pass, and have high quantum efficiency.

Accuracy with the LEO Raven hinges on mount tracking accuracy and stability. Plate solution distortion can be eliminated by using high resolution encoders which tell the mount where it points and decides the tracking rate of the mount. A very good encoder, typically 22 bits, will have a resolution of 0.3 arcseconds (360 degrees * 3600 seconds / 2^{22}). Stability of the telescope must seek to limit or accurately model the sage in the telescope and mount jitter when tracking. In addition, operating the LEO Raven in different environments introduces thermal issues and focus shifting of the telescope. These effects must be accounted for in the final LEO Raven model and design. With these issues considered, the LEO Raven can achieve an acceptable 5-10 arcsecond accuracy for doing astrometry.

The design considerations developed from this LEO Raven research, while providing powerful insight into future design, also introduce some new challenges. Incorporating these

design considerations into the LEO Raven will cause rising costs for the final system. Section 5.2 compares the cost of the current Raven system to the cost of a new LEO Raven system given these design inputs.

5.2 Cost Considerations

One of the stated goals of a Raven-class system is its low cost, commercial technology approach. Raven has operated since 1998, and overall costs are well understood. Current Oceanit estimates for the Raven hardware and commercial software are as follows[1]:

Ash Dome	$15K
Dome Automation	$10K
Software Bisque GT-1100 Mount	$15K
14.5” Telescope	$40K
Apogee AP-2 CCD camera	$15K
The Sky software	$1K
Telescope Control PC	$5K
Image Processing Workstation	$10K
Weather Station	$15K
Subtotal	$126K

Current estimates of a LEO Raven are as follows:

Dome	$15K
Dome Automation	$10K
Mount	$90K
1m Telescope	$40K
Optical Tube and Baffling	$40K
New Camera	$20K
The Sky software	$1K
Telescope Control PC	$5K
Image Processing Workstation	$10K
Weather Station	$15K
Subtotal	$246K

Given the current challenge of a LEO Raven design, the cost would be approximately twice that of the current Raven system. The 1m telescope, stable mount, and baffling will be expensive. In addition, the detector improvements might require some more monetary investment. Since the LEO Raven will be deployed, an alternative to the dome and dome controls might be found. This would reduce the cost of the system by about $25K. Although, this research answered many questions surrounding the design and performance of a LEO Raven, several areas exist for future research. These suggestions are explored in section 5.3.

5.3 Future Research

Future research could explore various atmospheric effects to include: polarization as a function of phase angle to the sun, filtering out the different absorption bands which contribute to the background noise, picking an entirely different spectral band pass, and worse case scenarios for transmission and sky radiance given a location. Other experiments must explore detector

improvements using the Indigo Phoenix detector or find a newer commercial detector in order for the LEO Raven to be successful. Additional star observations focusing on "solar-like" stars (G-class) having magnitudes ranging from about 4 to 8 during daylight could characterize the telescope/detector setup for collection of satellite passes. This LEO Raven research focused on K and M class stars which are better seen by the Indigo Merlin detector's 0.9-1.68 spectral band pass. Ultimately, LEO targets will be illuminated by the sun, a G2 star which peaks at about 0.49 microns, so this will be the characteristic reflected radiation observed for LEO satellites.

The following research recommendations stem from discussion in section 4.4. While the goal of completing daylight astrometry experiments with the DAS was not actually realized, several important things were learned in the process. Primarily, while a few stars would pass through the DAS FOV during the course of a pass, it would be desirable to have many more. This indicates that LEO Raven should attempt to incorporate a wider FOV, a more sensitive CCD, and maybe consider a 1m class optical system. Secondly, even with the above considerations, astrometry for the LEO Raven will likely be much more rudimentary than what is employed by the deep space Raven. With the deep space, visible sensors, the ten to hundreds of observed stars allow for the astrometric processing to directly estimate plate scale, orientation, and many other parameters for each image. For LEO Raven, many of these variables may have to be measured outside of the satellite track while only one to a small number of stars are available to calculate offsets from the nominal trajectory. Clearly, more astrometry experiments will be required in the future.[29]

5.4 Final Thoughts

At the conclusion of this LEO Raven risk reduction, the Air Force Research Laboratory, stands ready to move into further research and development of the deployable, LEO Raven. This system will undoubtedly attain the stated expectation of an inexpensive yet effective method to collect high accuracy metrics and photometry for LEO satellites outside of terminator. In addition, contributions to Air Force Space Commands space surveillance mission will be substantial since the current Ground-Based Electro-Optical Deep Space Surveillance (GEODSS) system only collects at night. This space surveillance mission area includes space object identification (SOI), threat assessments, and anomaly resolution. In addition, this new LEO Raven system will utilize a wider field of view and more sensitive detector which increases the neighborhood watch for space system protection, detects fainter objects, and aids in searching for new/lost/maneuvering objects. Adding the daylight capability also allows for worldwide coverage of daytime space launches. Overall, a LEO Raven system enhances Air Force Space Commands space surveillance mission and expands the High Accuracy Network Determination System (HANDS) to encompass not only GEO objects but LEO objects as well.

Appendix A: 0.42m HANDS Raven Pass List

Satellite #22781 Name: NAVSTAR 34 R/B(PAM-D) Designation: 1993-054C
Epoch time: 2003.10.21 04:21:16.754688
Inclination (degrees): 34.6504
Right ascension of ascending node (degrees): 179.7158
Eccentricity: 0.2412215
Argument of Perigee (degrees): 288.059
Mean anomaly (degrees): 47.3321
Mean motion (revs/day): 10.72781485

Sat #22781 at RME Raven from 2003-10-22 05:23 to 13:23 UTC

Time(UTC)	RA(hours)	Declination	dRA("/s)	dDec("/s)	Az	El	Range
05:51:48	18:18:25.68	+35:13:41.7	-177.055	-21.433	299.8	+46.4	5181.31
05:52:03	18:22:03.05	+35:08:05.5	-178.222	-23.235	299.8	+47.1	5149.40
05:52:18	18:25:41.58	+35:02:01.9	-179.394	-25.069	299.7	+47.8	5117.67
05:52:33	18:29:21.27	+34:55:30.6	-180.570	-26.935	299.7	+48.5	5086.11
05:52:48	18:33:02.09	+34:48:31.1	-181.749	-28.833	299.7	+49.2	5054.73
06:09:03	22:51:07.08	+06:39:38.3	-235.097	-169.606	128.6	+68.5	3853.75
06:09:18	22:55:03.55	+05:57:07.5	-235.004	-170.332	128.3	+67.4	3856.34
06:09:33	22:58:59.61	+05:14:26.6	-234.873	-170.955	128.1	+66.2	3859.80
06:09:48	23:02:55.24	+04:31:37.1	-234.704	-171.476	127.9	+65.1	3864.13
06:15:03	00:23:50.09	-10:16:15.6	-223.614	-159.955	125.7	+41.2	4157.45
06:15:18	00:27:37.22	-10:56:04.3	-222.813	-158.500	125.7	+40.1	4180.88
06:15:33	00:31:24.03	-11:35:30.8	-221.997	-156.985	125.6	+39.0	4205.14

Appendix B: 1.6m GEMINI Pass List

These were generated for the first observations on Oct 27-28.

Two Line Element set:

COSMOS 1606

1 15369U 84111A 03327.90758889 .00003592 00000-0 27935-3 0 7501

2 15369 82.5100 254.6049 0013295 283.6274 76.3469 15.00951307 34748

Observation Schedule for DAS collects:

Oct 27-28 Allocated times 0100-0400 UTC (1500-1600 Local)

Date	LRise	SON	UTC HBrk	UTC Rise	UTC Culm	UTC Set	Elev	Range
27-Oct-03	16:25	22195	2:06:17	2:25:00	2:42:32	3:00:15	52	6304.5
27-Oct-03	15:20	26977	23:10:27	1:20:46	4:50:14	6:17:21	83.6	12507
28-Oct-03	13:49	8820	23:32:36	23:49:36	0:05:32	0:21:50	50.5	6666.2
28-Oct-03	14:27	22195	0:10:19	0:27:43	0:49:28	1:10:51	87.3	5626.2
28-Oct-03	15:17	26977	23:06:53	1:17:28	4:50:21	6:19:29	85.2	12436
28-Oct-03	18:53	22824	4:48:37	4:53:45	4:56:03	4:58:22	50.8	999.5

Star-Fields

Mon		Sat	UTC	Az	Elev	Range
1st	Start	22195	2:21:56 Z	304.42	24.63	7886.8
Pass	Culm		2:42:32 Z	244.72	52	6304.8
	End		3:03:42 Z	181.2	24.11	7896.95
2nd	Start	26977	3:18:00 Z	127.12	60.16	33833.7
Pass	Culm		4:49:20 Z	69.23	83.58	24492.5
	End		6:20:50 Z	15.92	25.11	12170.8

Appendix C: 1.6m GEMINI Observations

11/7/03

Note that Maui is 10 hours ahead of UT.

UTC Time	Object	Notes	
2027-2029 UT	Sat 23560	Elev 31 degrees	
2030	Star 5695	Az 154, Elev 22	3.22 Mag
	Star 5107	Az 169 , Elev 68	3.37 Mag
2040	Sat 8820	Too high at 8,000 km	
2059-2104	Sat 25157	Elev 26.5	

Follow-up stars for the previous pass:

UTC Time	Object	Notes	
2110	Star 4434	Az 345, Elev 36	3.84 Mag
2115	Star 4782	Az 351, Elev 39	3.87 Mag
2133-2145	Sat 25398	Westpac	

Drift Star collects (turning off the tracker and allowing the earth's rotation to move the camera):

UTC Time	Object	Notes	
2200	Star 5191	Az 346, Elev 60	1.86 Mag
2205	Star 4911	Az 240, Elev 58	3.38 Mag

11/21/03

Local Time	Object	Notes
1248	Sat 25884	Try #1- No step, 30 sec
		Try #2- Stepped, 30 sec
		Try #3- Stepped, 20 sec
		Try #4- Stepped, 400 frames/sec
		Try #5- Stepped, 400 frames/sec
1258	Star 8465	20 degrees elevation
1300	Unsuccessful collects on Sat 503, 26065, 13073	
1309	Sat 13552	Try #7- Stepped, 20 sec
		Try #8- 2 steps, 20 sec lost target at 28 deg
1318	Sat 24836	Try #9, 20 sec 33 degrees down
		Try #10, 20 sec 27 down
		Star through FOV, 23 21 20
1327	Sat 15369	Try #11- stepped 20 sec
		Try #12- stepped 20 sec, 35 degrees down
		Try #13- stepped 20 sec
1337	Sat 18749	Try #14
		Try #15 Stars
	Try #16…hit stops	

Appendix D: 0.36m RME Raven Observations

11/12/03

Time	Object	Magnitude	Spectral Class
0915	62551	6.33	F6IV
	81298	2.0	K0III

No satellites were observed

11/14/03

Time	Object	Magnitude	Spectral Class	Integration Time
0845	14936	7.41	F0	10,000 micro sec
0850	Galaxy Observation			9,000 micro sec
0920	Unsuccessful tracking of Sat 27005u			
0935	Re-focused the telescope			
0937	30653	2.24	K5III	
1015	#22195	Unknown	Sunlit	5000-6000 micro sec
1020	#22195	No observation of the satellite		
1045	3073	9.60		
1055	Not seeing 5.41 mag stars #123353 (K-class)			
1057	102932	2.08	A5III	
1100	143021	3.43	B9V	2200 micro sec
1104	#22195			2500 micro sec

	#12295			1600 micro sec
1108	Vega	0.03	A0V	
1200	66485	3.86	K1II	5000 msec
1136	9087	3.55	F7V	

1140 Cloud cover limited observation

1143 Attempted Satellite: #23560

1150 Clouds came into view to the N, NE, and NW.

1200 Closed Dome

11/14/03 Night Observations

1840 Observed sat 26977

1850 Two Stars in the FOV in order to get an accurate plate scale in the event a successful satellite-star combination was collected.

	67309	4.67	F1V	16500 micro sec
	67315	4.59	A8V	
1900	125122	0.76	A7IV	
1915	67174	0.03	A0V	16500 micro sec

Bibliography

1. Sabol, C. Research Aerospace Engineer, Air Force Research Laboratory. "Air Force Maui Optical and Supercomputing Site Overview." Maui Space Surveillance Site, Maui, HI. 16 Dec 2002.

2. Sabol, C., K. Luu, P. Kervin, "Recent Developments of the Raven Small Telescope Program", AAS/AIAA Spaceflight Mechanics Conference, San Antonio, Texas, January 2002, AAS 02-131.

3. Sabol, C., et al, "SATEX: Satellite Tracking Experiment for High Accuracy Orbit Updates", AMOS Technical Conference, Maui, Hawaii, September 2002.

4. Sabol, C., K. Luu, K. Alfriend, "High Accuracy Orbit Updates using Angles-Only Data", AAS/AIAA Spaceflight Mechanics Conference, Maui, Hawaii, February 8-13, 2004, AAS 04-192.

5. Kelecy, T., C. Sabol, M. Murai, "High Accuracy Orbit Analysis Test Results using the High Accuracy Network Determination System (HANDS)," 2003 AMOS Technical Conference, Wailea, Maui, HI, September 9-13, 2003.

6. Sabol, C., T. Kelecy, M. Murai, "Geosynchronous Orbit Determination using the High Accuracy Network Determination System (HANDS)", AAS/AIAA Spaceflight Mechanics Conference, Maui, Hawaii, February 8-13, 2004, AAS 04-192.

7. Sabol, C. Research Aerospace Engineer, Air Force Research Laboratory. "Hands Review for DETC." Briefing to DETC. Maui Space Surveillance Site, Maui, HI. July 2003.

8. Evans, Howard and Ron Tuttle. Course notes, OENG 530, Introduction to IR and MASINT Phenomenology. School of Engineering and Management, Air Force Institute of Technology, Wright-Patterson AFB OH, Summer Quarter 2003.

9. IPAC. http://www.ipac.caltech.edu/Outreach/Edu/Regions/irregions.html

10. IR Windows. http://coolcosmos.ipac.caltech.edu/cosmic_classroom/ir_tutorial/irwindows.html

11. Elachi, Charles. Introduction to the Physics and Techniques of Remote Sensing. New York: Wiley-Interscience Publication, 1987; 47.

12. Smith, Warren J. Modern Optical Engineering. 2nd Ed. Massachusetts: McGraw-Hill, 1990.

13. Handbook of Geophysics and the Space Environment. Adolph S. Jursa, Editor. Air Force Geophysics Laboratory, AF Systems Command, USAF, 1985; 25-10.

14. GSU http://hyperphysics.phy-astr.gsu.edu/hbase/starlog/staspe.html

15. Coke. http://coke.physics.ucla.edu/laptag/Astro.dir/astrocls.dir/magscale.htm

16. Physics 519, course notes, Space Surveillance Notes. School of Engineering and Management, Air Force Institute of Technology, Wright-Patterson AFB OH, Winter Quarter 2003.

17. Evans, Howard and Ron Tuttle. Course notes, OENG 531, Nonimaging IR and MASINT Collection Systems. School of Engineering and Management, Air Force Institute of Technology, Wright-Patterson AFB OH, Summer Quarter 2003.

18. Rogalski, Antoni. "Infrared Detectors: An Overview." Infrared Physics & Technology 43 (2002): 187-210.

19. IPAC 2. http://www.ipac.caltech.edu/Outreach/Edu/ground.html

20. Chesser, D., "NIR Daylight Acquisition Sensor Improves Mission Capabilities", 2003 AMOS Technical Conference, Wailea, Maui, HI, September 9-13, 2003.

21. The Infrared Handbook. Ed. William L. Wolfe and George J. Zissis. 3rd Ed. Michigan: Infrared Information Analysis Center, 1989.

22. Mauna Kea Observatory. http://www.GEMINI.edu/sciops/ObsProcess/obsConstraints/ocSkyBackground.html

23. Schlessinger, Monroe Infrared Technology Fundamentals. 2nd Ed. New York: Marcel Dekker, Inc., 1995; 55.

24. Merlin User's guide

25. www.indigosystems.com

26. The Mauna Kea OH Line Emission Spectrum http://www.jach.hawaii.edu/JACpublic/UKIRT/instruments/cgs4/maunakea/ohlines.html

27. 2MASS. http://www.ipac.caltech.edu/2mass/release/allsky/doc/sec1_1.html Accessed 28 Oct 2003.

28. Zbyd, Jerry. Plexus Software, Release 3, Version 2. AFRL: June 2003.

29. Nelson, Joel, M. Goda, P. Sydney, C. Sabol, D. Talent, D. O'Connell, and M. Murai. "Daylight Astrometry and Design Studies for the LEO Raven." AAS/AIAA Spaceflight Mechanics Conference, Maui, Hawaii, February 8-13, 2004, AAS 04-192.

30. Sellers, Jerry. *Understanding Space: An Introduction to Astronautics.* Massachusetts: McGraw-Hill, 1994.

31. Smith, Warren J. *Modern Optical Engineering*. 2nd Ed. Massachusetts: McGraw-Hill, 1990.

Vita

Captain Joel E. Nelson graduated from Red River High School in Grand Forks, ND. He entered undergraduate studies at the United States Air Force Academy, Colorado Springs, Colorado where he graduated with a commission and Bachelor of Science degree in Physics (Astronomy) in June 1999.

His first assignment in August of 1999 was to the Air Force Research Laboratory's Directed Energy Directorate at Kirtland AFB. While in at AFRL he worked in the Satellite Assessment Center as an Optical Engineer. In June 2000, he was assigned to the Optical Surveillance SPO where he served as an executive officer and later as a physicist. While working in the Optical Surveillance SPO, he contributed to the success of a Secretary of Defense directed national-priority program relating to special access programs. In August 2002, he entered the Graduate School of Engineering and Management, Air Force Institute of Technology. Upon graduation, he will be assigned to the National Reconnaissance Office's Imagery Intelligence Directorate.

REPORT DOCUMENTATION PAGE	Form Approved OMB No. 074-0188

1. REPORT DATE *(DD-MM-YYYY)*	2. REPORT TYPE	3. DATES COVERED *(From – To)*
23 Mar 04	**Master's Thesis**	Feb 2003 – Mar 2004

4. TITLE AND SUBTITLE

INFRARED METHODS FOR DAYLIGHT ACQUISITON OF LEO SATELLITES

5a. CONTRACT NUMBER

5b. GRANT NUMBER

5c. PROGRAM ELEMENT NUMBER

6. AUTHOR(S)

Nelson, Joel E., Captain, USAF

5d. PROJECT NUMBER
If funded, enter ENR #

5e. TASK NUMBER

5f. WORK UNIT NUMBER

7. PERFORMING ORGANIZATION NAMES(S) AND ADDRESS(S)
Air Force Institute of Technology
Graduate School of Engineering and Management (AFIT/EN)
2950 Hobson Way, Building 640
WPAFB OH 45433-7765

8. PERFORMING ORGANIZATION REPORT NUMBER

AFIT/GSS/ENG/04-02

9. SPONSORING/MONITORING AGENCY NAME(S) AND ADDRESS(ES)
AFRL/DEBI, Det 15
Attn: Dr. Chris Sabol
535 Lipoa Parkway, Suite 200
Kihei, HI 96752 Comm:: (808) 874-1594

10. SPONSOR/MONITOR'S ACRONYM(S)

11. SPONSOR/MONITOR'S REPORT NUMBER(S)

12. DISTRIBUTION/AVAILABILITY STATEMENT
APPROVED FOR PUBLIC RELEASE; DISTRIBUTION UNLIMITED.

13. SUPPLEMENTARY NOTES

14. ABSTRACT

Raven is an award-winning optical system design paradigm that couples commercially available hardware and software along with custom data analysis and control software to produce low-cost, autonomous, and very capable space surveillance systems. The first product of the Raven program was a family of telescopes capable of generating world-class optical observation data of deep-space satellites. The key to this system was the use of astrometric techniques for position and brightness data. Astrometry compares a satellite to the star background within the sensor field of view; since the position and brightness of the star-field is well known in star catalogs, accurate knowledge of the satellite position and brightness can be deduced from this comparison. Efforts are now underway to produce a similar system capable of tracking low Earth orbiting (LEO) satellites: the LEO Raven. Tracking LEO objects presents several new challenges, most notably the speed of the satellite relative to the star-field and the lighting conditions. The current system works in the visible light band that requires terminator tracking conditions where the ground station is in the dark and the satellite is solar illuminated. Since this is not typically the case for LEO satellites, the first LEO Raven is being designed to use infrared light bands for daylight tracking. This thesis presents the results of risk-reduction daylight astrometry experiments using the Maui Space Surveillance Site's Daylight Acquisition Sensor.

15. SUBJECT TERMS
AMOS, Raven, LEO Raven, daylight sensing, optical sensor, SSA, satellite metric

16. SECURITY CLASSIFICATION OF:			17. LIMITATION OF ABSTRACT	18. NUMBER OF PAGES	19a. NAME OF RESPONSIBLE PERSON
REPORT	ABSTRACT	c. THIS PAGE			Matthew E. Goda, Maj, USAF (ENG)
U	U	U	UU	127	**19b. TELEPHONE NUMBER** *(Include area code)* (937) 255-6565, ext 4614; e-mail: Matthew.Goda@afit.edu

Standard Form 298 (Rev: 8-98)
Prescribed by ANSI Std. Z39-18

SF 298; Report Documentation Page